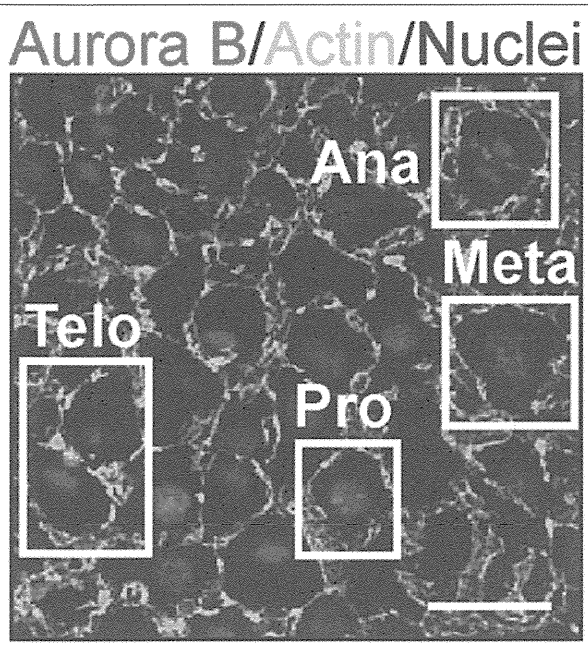

Figure 4 Hepatocytes in different stages of M phase distinguished by intracellular localization of Aurora B. A section of liver stained for Aurora B (red), actin (green), and nuclei (blue) is shown. The dynamic change in intracellular localization of Aurora B and nuclear morphology allow discrimination of hepatocytes in prophase (Pro), prometaphase/metaphase (Meta), anaphase (Ana), and telophase (Telo). Scale bar: 25 μm.

and binuclear cardiomyocytes seem to have distinct functions, and it has been proposed that only mononuclear cardiomyocytes maintain their proliferative potential to serve as stem or progenitor cells in heart muscle [79,80]. It is unclear whether hepatocytes with different numbers of nuclei have different functions. This issue is discussed further below.

A revised model of liver regeneration

Based on our findings, together with previous observations, we have proposed a revised model of liver regeneration [38]. Upon 30% PHx, the liver recovers its original mass by increasing the size of hepatocytes, but neither the cell number nor the nuclear number of hepatocytes changes. Furthermore, because only a small fraction of hepatocytes undergo S phase, their ploidy is not altered significantly (Figure 5A and Table 1). In contrast, when 70% of liver is removed, hypertrophy of hepatocytes occurs in a few hours after PHx, followed by cell proliferation. Almost all hepatocytes enter into S phase, but only about half undergoes cell division to increase their numbers. During proliferation, binuclear hepatocytes seem to preferentially undergo unconventional cell division, in which chromosomes from two nuclei are split into two nuclei to produce two mononuclear daughter hepatocytes. As a result, the nuclear number decreases, whereas ploidy increases (Figure 5B and Table 1). Although there are still some other possibilities to be considered, such as hepatocyte fusion and/or nuclear fusion during liver regeneration, we believe that this revised model represents the characteristic behavior of hepatocytes during liver regeneration and is more accurate than the traditional model.

Cellular robustness of hepatocytes

Adult hepatocytes can be binuclear, polyploid and even aneuploid under normal conditions [76,81]. Furthermore, cell number, cell size, nuclear number and ploidy of hepatocytes are significantly different in normal liver and regenerated liver after 30% or 70% PHx (Table 1). Despite these differences, liver seems to function almost equally in different conditions, which raises an intriguing question whether such differences in the cellular properties affect hepatocytes. One study using transcriptomic analysis showed that hepatocytes with different ploidy were basically indistinguishable [82]; however, another study indicated that polyploid cells were more resistant to stressful conditions [83]. Hepatocytes with different ploidy were shown to be equally susceptible to interferon-γ (IFN-γ)-induced apoptosis [84]. Proliferation of polyploid hepatocytes was compromised and they exhibited more characteristics of senescence [85]. No consensus has been reached on the functional differences in hepatocytes of different ploidy or number of nuclei. The volume of hepatocytes is basically proportional to their ploidy, which is often the case with other cell types [42,84,86,87]. However, we noticed that hepatocytes increase their size without increasing their DNA content after 30% PHx [38], suggesting that hypertrophy without increased ploidy allows hepatocytes to function properly. Naturally occurring aneuploidy is another feature of hepatocytes, which seems to arise from inaccurate chromosome segregation [76,81]. Aneuploidy is often associated with genetic disorders and is observed in various cancers [88,89]. However, aneuploidy does not seem to be tumorigenic in hepatocytes, and it may even provide genetic diversity in hepatocytes to perform different functions [81].

In addition to these characteristic features exhibited by wild-type mice, genetically modified mice show rather extreme phenotypes of hepatocytes. Mutant mice with impaired cell cycle progression showed a fully functional liver with extraordinarily enlarged hepatocytes after 70% PHx [44-47]. A loss of E2F7 and E2F8 reduced ploidy or nuclear number but did not affect hepatocyte function and regeneration after several liver injuries including PHx [67,68]. Furthermore, hepatocytes were resistant to DNA damage caused by a lack of telomeric repeat binding factor 2 (TRF2). In the absence of TRF2, liver regenerated by increasing the size and ploidy of hepatocytes and was fully functional after 70% PHx [90]. These observations indicate collectively that hepatocytes have a

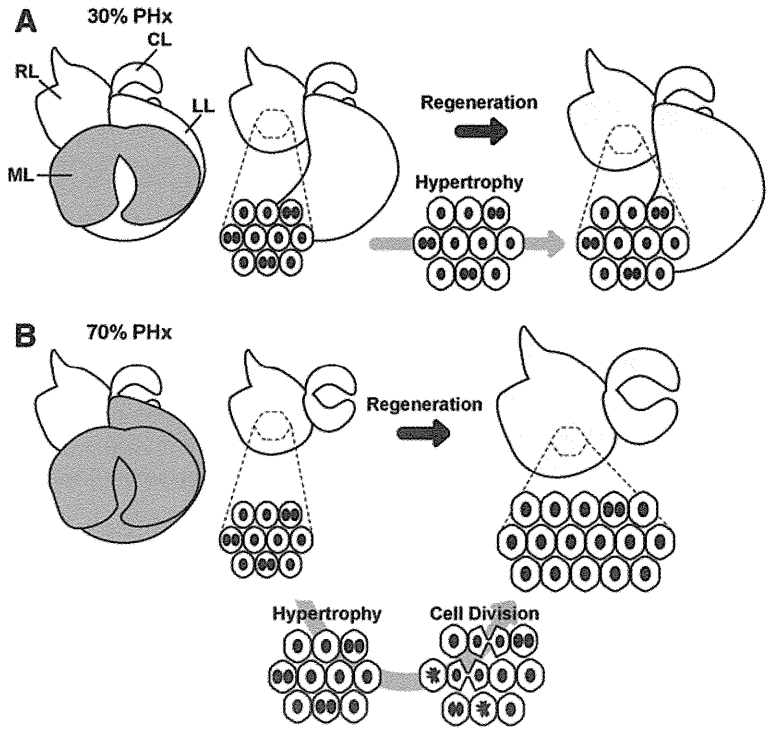

Figure 5 The revised model of liver regeneration. (**A**) Liver regeneration after 30% PHx. The median lobe (ML) is removed and the left lobe (LL), right lobe (RL), and caudate lobe (CL) regrow. During this process, all hepatocytes enlarge, but some enter S phase and divide only rarely. As a result, hepatocytes slightly increase their ploidy, but do not change their nuclear number. (**B**) Liver regeneration after 70% PHx. All hepatocytes increase their size and then enter the cell cycle to undergo S phase. Some cells execute cell division to produce mainly mononuclear daughter hepatocytes, irrespective of nuclear number of mother hepatocytes. However, not all hepatocytes divide. Liver recovers its lost mass by a combination of hypertrophy and proliferation. As a result, hepatocytes increase their ploidy, but decrease their nuclear number.

"cellular robustness" which allows them to perform their functions in a variety of settings; these differ in terms of cell size, ploidy or nuclear number. The observed extreme plasticity in ploidy of hepatocytes supports their robustness [76]. It is tempting to speculate that the cellular robustness of hepatocytes is one reason why of mammalian organs, only the liver has such a marked regenerative capacity.

Size control of organs

Liver regeneration serves as an excellent model for regulation of organ size. Generally, differences in organ size among animals reflect differences in cell number rather than cell size [91,92]. Limb regeneration in amphibians also depends on an increase in cell number to fully recover the original tissues. However, the size and number of hepatocytes in liver regeneration after PHx contribute differentially to the recovery of liver mass. It has been suggested that removal of one kidney induces the enlargement of the other by increasing the size of kidney cells [93]. Moreover, physiological and pathological cardiac hyperplasia is induced by hypertrophy of cardiomyocytes [94,95]. Therefore, cellular hypertrophy could be a general mechanism for increasing organ size. Hippo/mammalian Ste-20 like kinase (Mst)1/2-Yorkie/Yes-associated protein (YAP) signaling plays an indispensable role in the regulation of organ size [96-99]. In normal adult hepatocytes, Mst1/2 kinase (the mammalian homologue of *Drosophila* Hippo) phosphorylates and inactivates YAP (the mammalian homologue of *Drosophila* Yorkie), which is a transcription activator that induces cell proliferation and suppresses apoptosis. Transgenic expression of human YAP in mouse hepatocytes drastically increased the liver size [96]. This regulation of organ size by Hippo/Mst1/2-Yorkie/YAP signaling might be due mainly to the control of proliferation and apoptosis in cells [100]. However, Hippo/Mst1/2-Yorkie/YAP signaling affects cell size by tuning Akt-mTOR signaling via miRNA [101], demonstrating that cell size plays a critical role in organ size regulation by Hippo/Mst1/2-Yorkie/YAP signaling as well.

Table 1 Cellular properties of hepatocytes in regenerated liver after 30 and 70% PHx, compared to normal liver

	Cell number	Cell size	Nuclear number	Ploidy
30% PHx	Decreased	Increased	Unchanged	Marginally increased
70% PHx	Decreased	Increased	Decreased	Increased

What senses and regulates liver size is a fundamental question. The decreased number of hepatocytes and increased size of hepatocytes in regenerated liver suggests that liver size is determined by the total mass of hepatocytes. PHx drastically changes the blood flow into the liver. This increased blood flow generates shear stress that induces nitric oxide production, triggering regeneration [102-106]. In addition, the amount of bile acid in the blood might serve as a mechanism of monitoring the size of liver because it reflects the total mass of the hepatocytes [107,108]. Additionally, because the liver serves as a major reservoir of glycogen, the blood glucose level reflects the liver mass and so might also be a sensor. Consistent with this hypothesis, it has long been known that rodents become hypoglycemic after PHx, and supplementation of glucose inhibits liver regeneration [109-111]. This inhibitory effect of glucose is suggested to be mediated by p21 [112]. Other factors in the regulation of liver size might be cytokines and serum proteins secreted from hepatocytes. A key contributing feature of these factors is that they must reflect the total mass of hepatocytes, but not the number or size of individual hepatocytes. Although these factors may sense the liver size, the mechanism of initiating and promoting regenerative responses remains unknown. Furthermore, liver regeneration must terminate when the liver recovers its original mass. Several molecules have been suggested to be involved in the termination of liver regeneration including transforming growth factor-β (TGF-β), a mitoinhibitory cytokine for hepatocytes [113]; extracellular matrix, which might inhibit proliferation of hepatocytes via integrin-linked kinase (ILK) and glypican 3 [114-116]; and peroxisome prol iferator-activated receptor-γ (PPAR-γ) a mitoinhibitory transcription factor for hepatocytes [117]. However, the termination of liver regeneration has been inadequately studied compared to the initiation process. Recent transcriptome analyses of termination may shed light on its underlying molecular mechanisms [118,119]. A future challenge is to elucidate the molecular links between the sensors of liver size, the factors that regulate the hypertrophic and proliferative responses of hepatocytes, and the termination process of liver regeneration that acts to maintain the appropriate liver size.

Conclusions

Although liver regeneration has been studied extensively, many important fundamental mechanisms remain undefined such as the mechanisms of cellular hypertrophy, cell division, nuclear division, ploidy changes and organ size control. Liver regeneration after PHx provides an excellent experimental system to tackle such basic biological questions. Understanding the mechanisms underlying liver regeneration is clinically important because hepatectomy is a practical treatment for liver tumors, and liver transplantation is an important therapeutic option in patients with severe liver diseases. Understanding the mechanism of liver regeneration will lead to the development of promising therapeutic strategies.

Competing interests

The authors declare that they have no competing interests.

Authors' contributions

YM and AM wrote the manuscript. YM prepared the figures and table. Both authors read and approved the final manuscript.

Acknowledgements

We thank Dr. T. Itoh for his critical reading of this manuscript. YM is a recipient of a JSPS Postdoctoral Fellowship for Research Abroad and an Uehara Memorial Foundation Research Fellowship. This work was supported in part by research grants to AM from the Ministry of Education, Culture, Sports, Science and Technology of Japan, Ministry of Health, Labour and Welfare of Japan, and the CREST program from Japan Science and Technology Agency.

Author details

[1]Laboratory of Cell Growth and Differentiation, Institute of Molecular and Cellular Biosciences, The University of Tokyo, Yayoi, Bunkyo-ku, Tokyo 113-0032, Japan. [2]Current address: Gladstone Institute of Cardiovascular Disease, University of California at San Francisco, San Francisco, CA 94158, USA.

Received: 6 June 2013 Accepted: 17 June 2013
Published: 20 June 2013

References

1. Palmes D, Spiegel HU: **Animal models of liver regeneration.** *Biomaterials* 2004, **25**:1601–1611.
2. Alison MR, Islam S, Lim S: **Stem cells in liver regeneration, fibrosis and cancer: the good, the bad and the ugly.** *J Pathol* 2009, **217**:282–298.
3. Si-Tayeb K, Lemaigre FP, Duncan SA: **Organogenesis and development of the liver.** *Dev Cell* 2010, **18**:175–189.
4. Zaret KS, Grompe M: **Generation and regeneration of cells of the liver and pancreas.** *Science* 2008, **322**:1490–1494.
5. Tanaka M, Itoh T, Tanimizu N, Miyajima A: **Liver stem/progenitor cells: their characteristics and regulatory mechanisms.** *J Biochem* 2011, **149**:231–239.
6. Court FG, Wemyss-Holden SA, Dennison AR, Maddern GJ: **The mystery of liver regeneration.** *Br J Surg* 2002, **89**:1089–1095.
7. Fausto N: **Liver regeneration.** *J Hepatol* 2000, **32**:19–31.
8. Michalopoulos GK: **Liver regeneration.** *J Cell Physiol* 2007, **213**:286–300.
9. Michalopoulos GK, DeFrances M: **Liver regeneration.** *Adv Biochem Eng Biotechnol* 2005, **93**:101–134.
10. Brockes JP, Kumar A: **Comparative aspects of animal regeneration.** *Annu Rev Cell Dev Biol* 2008, **24**:525–549.
11. Milne LS: **The histology of liver tissue regeneration.** *J Pathol Bacteriol* 1909, **13**:127–160.
12. Higgins G, Anderson GM: **Experimental pathology of the liver. Restoration of the liver of the white rat following partial surgical removal.** *Arch Pathol* 1931, **12**:186–202.
13. Beams HW, King RL: **The origin of binucleate and large mono nucleate cells in the liver of the rat.** *Anat Rec* 1942, **83**:281–297.
14. Sulkin NM: **A study of the nucleus in the normal and hyperplastic liver of the rat.** *Am J Anat* 1943, **73**:107–125.
15. St Aubin PM, Bucher NL: **A study of binucleate cell counts in resting and regenerating rat liver employing a mechanical method for the separation of liver cells.** *Anat Rec* 1952, **112**:797–809.
16. Jordan SW: **Electron Microscopy of Hepatic Regeneration.** *Exp Mol Pathol* 1964, **86**:183–200.
17. Stenger RJ, Confer DB: **Hepatocellular ultrastructure during liver regeneration after subtotal hepatectomy.** *Exp Mol Pathol* 1966, **5**:455–474.
18. Aterman K: **Electron microscopy of the rat liver cell after partial hepatectomy.** *J Pathol Bacteriol* 1961, **82**:367–369.

19. Fisher ER, Fisher B: **Ultrastructural Hepatic Changes Following Partial Hepatectomy and Portacaval Shunt in the Rat.** *Lab Invest* 1963, **12**:929–942.
20. Grisham JW: **A morphologic study of deoxyribonucleic acid synthesis and cell proliferation in regenerating rat liver; autoradiography with thymidine-H3.** *Cancer Res* 1962, **22**:842–849.
21. Bucher NL, Swaffield MN: **The Rate of Incorporation of Labeled Thymidine into the Deoxyribonucleic Acid of Regenerating Rat Liver in Relation to the Amount of Liver Excised.** *Cancer Res* 1964, **24**:1611–1625.
22. Fabrikant JI: **The kinetics of cellular proliferation in regenerating liver.** *J Cell Biol* 1968, **36**:551–565.
23. Bucher NL, Swaffield MN: **Rate of incorporation of [6-14C]orotic acid into uridine 5'-triphosphate and cytidine 5'-triphosphate and nuclear ribonucleic acid in regenerating rat liver.** *Biochim Biophys Acta* 1965, **108**:551–567.
24. Bucher NL, Oakman NJ: **Thymidine triphosphate content of regenerating rat liver.** *Biochim Biophys Acta* 1969, **186**:13–20.
25. Stocker E, Pfeifer U: **[On the manner of proliferation of the liver parenchyma after partial hepatectomy. Autoradiography studies using 3H-thymidine].** *Naturwissenschaften* 1965, **52**:663.
26. Fausto N, Campbell JS, Riehle KJ: **Liver regeneration.** *Hepatology* 2006, **43**:S45–S53.
27. Duncan AW, Dorrell C, Grompe M: **Stem cells and liver regeneration.** *Gastroenterology* 2009, **137**:466–481.
28. Koller BH, Hagemann LJ, Doetschman T, Hagaman JR, Huang S, Williams PJ, First NL, Maeda N, Smithies O: **Germ-line transmission of a planned alteration made in a hypoxanthine phosphoribosyltransferase gene by homologous recombination in embryonic stem cells.** *Proc Natl Acad Sci USA* 1989, **86**:8927–8931.
29. Schwartzberg PL, Goff SP, Robertson EJ: **Germ-line transmission of a c-abl mutation produced by targeted gene disruption in ES cells.** *Science* 1989, **246**:799–803.
30. Thompson S, Clarke AR, Pow AM, Hooper ML, Melton DW: **Germ line transmission and expression of a corrected HPRT gene produced by gene targeting in embryonic stem cells.** *Cell* 1989, **56**:313–321.
31. Tan X, Behari J, Cieply B, Michalopoulos GK, Monga SP: **Conditional deletion of beta-catenin reveals its role in liver growth and regeneration.** *Gastroenterology* 2006, **131**:1561–1572.
32. Chen L, Zeng Y, Yang H, Lee TD, French SW, Corrales FJ, Garcia-Trevijano ER, Avila MA, Mato JM, Lu SC: **Impaired liver regeneration in mice lacking methionine adenosyltransferase 1A.** *FASEB J* 2004, **18**:914–916.
33. Nakamura K, Nonaka H, Saito H, Tanaka M, Miyajima A: **Hepatocyte proliferation and tissue remodeling is impaired after liver injury in oncostatin M receptor knockout mice.** *Hepatology* 2004, **39**:635–644.
34. Beyer TA, Xu W, Teupser D, Auf Dem Keller U, Bugnon P, Hildt E, Thiery J, Kan YW, Werner S: **Impaired liver regeneration in Nrf2 knockout mice: role of ROS-mediated insulin/IGF-1 resistance.** *EMBO J* 2008, **27**:212–223.
35. Factor VM, Seo D, Ishikawa T, Kaposi-Novak P, Marquardt JU, Andersen JB, Conner EA, Thorgeirsson SS: **Loss of c-Met disrupts gene expression program required for G2/M progression during liver regeneration in mice.** *PLoS One* 2010, **5**:e12739.
36. Geschwind II, Alfert M, Schooley C: **Liver regeneration and hepatic polyploidy in the hypophysectomized rat.** *Exp Cell Res* 1958, **15**:232–235.
37. Gentric G, Celton-Morizur S, Desdouets C: **Polyploidy and liver proliferation.** *Clin Res Hepatol Gastroenterol* 2012, **36**:29–34.
38. Miyaoka Y, Ebato K, Kato H, Arakawa S, Shimizu S, Miyajima A: **Hypertrophy and unconventional cell division of hepatocytes underlie liver regeneration.** *Curr Biol* 2012, **22**:1166–1175.
39. Herweijer H, Wolff JA: **Gene therapy progress and prospects: hydrodynamic gene delivery.** *Gene Ther* 2007, **14**:99–107.
40. Wooddell CI, Reppen T, Wolff JA, Herweijer H: **Sustained liver-specific transgene expression from the albumin promoter in mice following hydrodynamic plasmid DNA delivery.** *J Gene Med* 2008, **10**:551–563.
41. Mitchell C, Nivison M, Jackson LF, Fox R, Lee DC, Campbell JS, Fausto N: **Heparin-binding epidermal growth factor-like growth factor links hepatocyte priming with cell cycle progression during liver regeneration.** *J Biol Chem* 2005, **280**:2562–2568.
42. Conlon I, Raff M: **Size control in animal development.** *Cell* 1999, **96**:235–244.
43. Su AI, Guidotti LG, Pezacki JP, Chisari FV, Schultz PG: **Gene expression during the priming phase of liver regeneration after partial hepatectomy in mice.** *Proc Natl Acad Sci USA* 2002, **99**:11181–11186.
44. Haga S, Ogawa W, Inoue H, Terui K, Ogino T, Igarashi R, Takeda K, Akira S, Enosawa S, Furukawa H, *et al*: **Compensatory recovery of liver mass by Akt-mediated hepatocellular hypertrophy in liver-specific STAT3-deficient mice.** *J Hepatol* 2005, **43**:799–807.
45. Minamishima YA, Nakayama K: **Recovery of liver mass without proliferation of hepatocytes after partial hepatectomy in Skp2-deficient mice.** *Cancer Res* 2002, **62**:995–999.
46. Wirth KG, Wutz G, Kudo NR, Desdouets C, Zetterberg A, Taghybeeglu S, Seznec J, Ducos GM, Ricci R, Firnberg N, *et al*: **Separase: a universal trigger for sister chromatid disjunction but not chromosome cycle progression.** *J Cell Biol* 2006, **172**:847–860.
47. Diril MK, Ratnacaram CK, Padmakumar VC, Du T, Wasser M, Coppola V, Tessarollo L, Kaldis P: **Cyclin-dependent kinase 1 (Cdk1) is essential for cell division and suppression of DNA re-replication but not for liver regeneration.** *Proc Natl Acad Sci USA* 2012, **109**:3826–3831.
48. Nagy P, Teramoto T, Factor VM, Sanchez A, Schnur J, Paku S, Thorgeirsson SS: **Reconstitution of liver mass via cellular hypertrophy in the rat.** *Hepatology* 2001, **33**:339–345.
49. Trotter NL: **A Fine Structure Study of Lipid in Mouse Liver Regenerating after Partial Hepatectomy.** *J Cell Biol* 1964, **21**:233–244.
50. Trotter NL: **Electron-opaque, lipid-containing bodies in mouse liver at early intervals after partial hepatectomy and sham operation.** *J Cell Biol* 1965, **25**(Suppl):41–52.
51. Shteyer E, Liao Y, Muglia LJ, Hruz PW, Rudnick DA: **Disruption of hepatic adipogenesis is associated with impaired liver regeneration in mice.** *Hepatology* 2004, **40**:1322–1332.
52. Murray AB, Strecker W, Silz S: **Ultrastructural changes in rat hepatocytes after partial hepatectomy, and comparison with biochemical results.** *J Cell Sci* 1981, **50**:433–448.
53. Kozma SC, Thomas G: **Regulation of cell size in growth, development and human disease: PI3K, PKB and S6K.** *Bioessays* 2002, **24**:65–71.
54. Kim S, Li Q, Dang CV, Lee LA: **Induction of ribosomal genes and hepatocyte hypertrophy by adenovirus-mediated expression of c-Myc in vivo.** *Proc Natl Acad Sci USA* 2000, **97**:11198–11202.
55. Beer S, Zetterberg A, Ihrie RA, McTaggart RA, Yang Q, Bradon N, Arvanitis C, Attardi LD, Feng S, Ruebner B, *et al*: **Developmental context determines latency of MYC-induced tumorigenesis.** *PLoS Biol* 2004, **2**:e332.
56. Baena E, Gandarillas A, Vallespinos M, Zanet J, Bachs O, Redondo C, Fabregat I, Martinez AC, De Alboran IM: **c-Myc regulates cell size and ploidy but is not essential for postnatal proliferation in liver.** *Proc Natl Acad Sci USA* 2005, **102**:7286–7291.
57. Ruvinsky I, Meyuhas O: **Ribosomal protein S6 phosphorylation: from protein synthesis to cell size.** *Trends Biochem Sci* 2006, **31**:342–348.
58. Jorgensen P, Tyers M: **How cells coordinate growth and division.** *Curr Biol* 2004, **14**:R1014–R1027.
59. Gentric G, Desdouets C, Celton-Morizur S: **Hepatocytes polyploidization and cell cycle control in liver physiopathology.** *Int J Hepatol* 2012, **2012**:282430.
60. Celton-Morizur S, Merlen G, Couton D, Desdouets C: **Polyploidy and liver proliferation: central role of insulin signaling.** *Cell Cycle* 2010, **9**:460–466.
61. Celton-Morizur S, Merlen G, Couton D, Margall-Ducos G, Desdouets C: **The insulin/Akt pathway controls a specific cell division program that leads to generation of binucleated tetraploid liver cells in rodents.** *J Clin Invest* 2009, **119**:1880–1887.
62. Satyanarayana A, Wiemann SU, Buer J, Lauber J, Dittmar KEJ, Wustefeld T, Blasco MA, Manns MP, Rudolph KL: **Telomere shortening impairs organ regeneration by inhibiting cell cycle re-entry of a subpopulation of cells.** *EMBO J* 2003, **22**:4003–4013.
63. Enserink JM, Kolodner RD: **An overview of Cdk1-controlled targets and processes.** *Cell Div* 2010, **5**:11.
64. Bloom J, Cross FR: **Multiple levels of cyclin specificity in cell-cycle control.** *Nat Rev Mol Cell Biol* 2007, **8**:149–160.
65. Norbury C, Blow J, Nurse P: **Regulatory phosphorylation of the p34cdc2 protein kinase in vertebrates.** *EMBO J* 1991, **10**:3321–3329.
66. Lee HO, Davidson JM, Duronio RJ: **Endoreplication: polyploidy with purpose.** *Genes Dev* 2009, **23**:2461–2477.

67. Chen HZ, Ouseph MM, Li J, Pecot T, Chokshi V, Kent L, Bae S, Byrne M, Duran C, Comstock G, *et al*: **Canonical and atypical E2Fs regulate the mammalian endocycle.** *Nat Cell Biol* 2012, **14**:1192–1202.
68. Pandit SK, Westendorp B, Nantasanti S, Van Liere E, Tooten PC, Cornelissen PW, Toussaint MJ, Lamers WH, de Bruin A: **E2F8 is essential for polyploidization in mammalian cells.** *Nat Cell Biol* 2012, **14**:1181–1191.
69. Harrison MF: **Percentage of binucleate cells in the livers of adult rats.** *Nature* 1953, **171**:611.
70. Wheatley DN: **Binucleation in mammalian liver. Studies on the control of cytokinesis in vivo.** *Exp Cell Res* 1972, **74**:455–465.
71. Gerlyng P, Abyholm A, Grotmol T, Erikstein B, Huitfeldt HS, Stokke T, Seglen PO: **Binucleation and polyploidization patterns in developmental and regenerative rat liver growth.** *Cell Prolif* 1993, **26**:557–565.
72. Yu JT, Foster RG, Dean DC: **Transcriptional repression by RB-E2F and regulation of anchorage-independent survival.** *Mol Cell Biol* 2001, **21**:3325–3335.
73. Brennan P, Babbage JW, Burgering BM, Groner B, Reif K, Cantrell DA: **Phosphatidylinositol 3-kinase couples the interleukin-2 receptor to the cell cycle regulator E2F.** *Immunity* 1997, **7**:679–689.
74. Ruchaud S, Carmena M, Earnshaw WC: **Chromosomal passengers: conducting cell division.** *Nat Rev Mol Cell Biol* 2007, **8**:798–812.
75. Guidotti JE, Bregerie O, Robert A, Debey P, Brechot C, Desdouets C: **Liver cell polyploidization: a pivotal role for binuclear hepatocytes.** *J Biol Chem* 2003, **278**:19095–19101.
76. Duncan AW, Taylor MH, Hickey RD, Hanlon Newell AE, Lenzi ML, Olson SB, Finegold MJ, Grompe M: **The ploidy conveyor of mature hepatocytes as a source of genetic variation.** *Nature* 2010, **467**:707–710.
77. Thornburg K, Jonker S, O'Tierney P, Chattergoon N, Louey S, Faber J, Giraud G: **Regulation of the cardiomyocyte population in the developing heart.** *Prog Biophys Mol Biol* 2011, **106**:289–299.
78. Liu Z, Yue S, Chen X, Kubin T, Braun T: **Regulation of cardiomyocyte polyploidy and multinucleation by CyclinG1.** *Circ Res* 2010, **106**:1498–1506.
79. Sedmera D, Thompson RP: **Myocyte proliferation in the developing heart.** *Dev Dyn* 2011, **240**:1322–1334.
80. Bersell K, Arab S, Haring B, Kuhn B: **Neuregulin1/ErbB4 signaling induces cardiomyocyte proliferation and repair of heart injury.** *Cell* 2009, **138**:257–270.
81. Duncan AW, Hanlon Newell AE, Smith L, Wilson EM, Olson SB, Thayer MJ, Strom SC, Grompe M: **Frequent aneuploidy among normal human hepatocytes.** *Gastroenterology* 2012, **142**:25–28.
82. Lu P, Prost S, Caldwell H, Tugwood JD, Betton GR, Harrison DJ: **Microarray analysis of gene expression of mouse hepatocytes of different ploidy.** *Mamm Genome* 2007, **18**:617–626.
83. Anatskaya OV, Vinogradov AE: **Genome multiplication as adaptation to tissue survival: evidence from gene expression in mammalian heart and liver.** *Genomics* 2007, **89**:70–80.
84. Martin NC, McCullough CT, Bush PG, Sharp L, Hall AC, Harrison DJ: **Functional analysis of mouse hepatocytes differing in DNA content: volume, receptor expression, and effect of IFNgamma.** *J Cell Physiol* 2002, **191**:138–144.
85. Sigal SH, Rajvanshi P, Gorla GR, Sokhi RP, Saxena R, Gebhard DR Jr, Reid LM, Gupta S: **Partial hepatectomy-induced polyploidy attenuates hepatocyte replication and activates cell aging events.** *Am J Physiol* 1999, **276**:G1260–G1272.
86. Fankhauser G: **Maintenance of normal structure in heteroploid salamander larvae, through compensation of changes in cell size by adjustment of cell number and cell shape.** *J Exp Zool* 1945, **100**:445–455.
87. Henery CC, Bard JB, Kaufman MH: **Tetraploidy in mice, embryonic cell number, and the grain of the developmental map.** *Dev Biol* 1992, **152**:233–241.
88. Holland AJ, Cleveland DW: **Losing balance: the origin and impact of aneuploidy in cancer.** *EMBO Rep* 2012, **13**:501–514.
89. Pfau SJ, Amon A: **Chromosomal instability and aneuploidy in cancer: from yeast to man.** *EMBO Rep* 2012, **13**:515–527.
90. Lazzerini Denchi E, Celli G, de Lange T: **Hepatocytes with extensive telomere deprotection and fusion remain viable and regenerate liver mass through endoreduplication.** *Genes Dev* 2006, **20**:2648–2653.
91. Raff MC: **Size control: the regulation of cell numbers in animal development.** *Cell* 1996, **86**:173–175.
92. Savage VM, Allen AP, Brown JH, Gillooly JF, Herman AB, Woodruff WH, West GB: **Scaling of number, size, and metabolic rate of cells with body size in mammals.** *Proc Natl Acad Sci USA* 2007, **104**:4718–4723.
93. Liu B, Preisig PA: **Compensatory renal hypertrophy is mediated by a cell cycle-dependent mechanism.** *Kidney Int* 2002, **62**:1650–1658.
94. Harvey PA, Leinwand LA: **The cell biology of disease: cellular mechanisms of cardiomyopathy.** *J Cell Biol* 2011, **194**:355–365.
95. Watkins H, Ashrafian H, Redwood C: **Inherited cardiomyopathies.** *N Engl J Med* 2011, **364**:1643–1656.
96. Dong J, Feldmann G, Huang J, Wu S, Zhang N, Comerford SA, Gayyed MF, Anders RA, Maitra A, Pan D: **Elucidation of a universal size-control mechanism in Drosophila and mammals.** *Cell* 2007, **130**:1120–1133.
97. Song H, Mak KK, Topol L, Yun K, Hu J, Garrett L, Chen Y, Park O, Chang J, Simpson RM, *et al*: **Mammalian Mst1 and Mst2 kinases play essential roles in organ size control and tumor suppression.** *Proc Natl Acad Sci USA* 2010, **107**:1431–1436.
98. Tumaneng K, Russell RC, Guan KL: **Organ size control by Hippo and TOR pathways.** *Curr Biol* 2012, **22**:R368–R379.
99. Pan D: **Hippo signaling in organ size control.** *Genes Dev* 2007, **21**:886–897.
100. Tordjmann T: **Hippo signalling: liver size regulation and beyond.** *Clin Res Hepatol Gastroenterol* 2011, **35**:344–346.
101. Tumaneng K, Schlegelmilch K, Russell RC, Yimlamai D, Basnet H, Mahadevan N, Fitamant J, Bardeesy N, Camargo FD, Guan KL: **YAP mediates crosstalk between the Hippo and PI(3)K-TOR pathways by suppressing PTEN via miR-29.** *Nat Cell Biol* 2012, **14**:1322–1329.
102. Wang HH, Lautt WW: **Evidence of nitric oxide, a flow-dependent factor, being a trigger of liver regeneration in rats.** *Can J Physiol Pharmacol* 1998, **76**:1072–1079.
103. Schoen JM, Wang HH, Minuk GY, Lautt WW: **Shear stress-induced nitric oxide release triggers the liver regeneration cascade.** *Nitric Oxide* 2001, **5**:453–464.
104. Macedo MP, Lautt WW: **Shear-induced modulation of vasoconstriction in the hepatic artery and portal vein by nitric oxide.** *Am J Physiol* 1998, **274**:G253–G260.
105. Sato Y, Tsukada K, Hatakeyama K: **Role of shear stress and immune responses in liver regeneration after a partial hepatectomy.** *Surg Today* 1999, **29**:1–9.
106. Niiya T, Murakami M, Aoki T, Murai N, Shimizu Y, Kusano M: **Immediate increase of portal pressure, reflecting sinusoidal shear stress, induced liver regeneration after partial hepatectomy.** *J Hepatobiliary Pancreat Surg* 1999, **6**:275–280.
107. Huang W, Ma K, Zhang J, Qatanani M, Cuvillier J, Liu J, Dong B, Huang X, Moore DD: **Nuclear receptor-dependent bile acid signaling is required for normal liver regeneration.** *Science* 2006, **312**:233–236.
108. Meng Z, Liu N, Fu X, Wang X, Wang YD, Chen WD, Zhang L, Forman BM, Huang W: **Insufficient bile acid signaling impairs liver repair in CYP27(−/−) mice.** *J Hepatol* 2011, **55**:885–895.
109. Holecek M: **Nutritional modulation of liver regeneration by carbohydrates, lipids, and amino acids: a review.** *Nutrition* 1999, **15**:784–788.
110. Simek J, Chmelar V, Melka J, Pazderka, Charvat Z: **Influence of protracted infusion of glucose and insulin on the composition and regeneration activity of liver after partial hepatectomy in rats.** *Nature* 1967, **213**:910–911.
111. Simek J, Melka J, Pospisil M, Neradilkova M: **Effect of protracted glucose infusion on the development of early biochemical changes and initiation of regeneration in rat liver after partial hepatectomy.** *Physiol Bohemoslov* 1965, **14**:366–370.
112. Weymann A, Hartman E, Gazit V, Wang C, Glauber M, Turmelle Y, Rudnick DA: **p21 is required for dextrose-mediated inhibition of mouse liver regeneration.** *Hepatology* 2009, **50**:207–215.
113. Carr BI, Hayashi I, Branum EL, Moses HL: **Inhibition of DNA synthesis in rat hepatocytes by platelet-derived type beta transforming growth factor.** *Cancer Res* 1986, **46**:2330–2334.
114. Apte U, Gkretsi V, Bowen WC, Mars WM, Luo JH, Donthamsetty S, Orr A, Monga SP, Wu C, Michalopoulos GK: **Enhanced liver regeneration following changes induced by hepatocyte-specific genetic ablation of integrin-linked kinase.** *Hepatology* 2009, **50**:844–851.
115. Liu B, Bell AW, Paranjpe S, Bowen WC, Khillan JS, Luo JH, Mars WM, Michalopoulos GK: **Suppression of liver regeneration and hepatocyte**

proliferation in hepatocyte-targeted glypican 3 transgenic mice. *Hepatology* 2010, **52**:1060–1067.
116. Liu B, Paranjpe S, Bowen WC, Bell AW, Luo JH, Yu YP, Mars WM, Michalopoulos GK: **Investigation of the role of glypican 3 in liver regeneration and hepatocyte proliferation.** *Am J Pathol* 2009, **175**:717–724.
117. Yamamoto Y, Ono T, Dhar DK, Yamanoi A, Tachibana M, Tanaka T, Nagasue N: **Role of peroxisome proliferator-activated receptor-gamma (PPARgamma) during liver regeneration in rats.** *J Gastroenterol Hepatol* 2008, **23**:930–937.
118. Nygard IE, Mortensen KE, Hedegaard J, Conley LN, Kalstad T, Bendixen C, Revhaug A: **The genetic regulation of the terminating phase of liver regeneration.** *Comp Hepatol* 2012, **11**:3.
119. Rychtrmoc D, Hubalkova L, Viskova A, Libra A, Buncek M, Cervinkova Z: **Transcriptome temporal and functional analysis of liver regeneration termination.** *Physiol Res* 2012, **61**(Suppl 2):S77–S92.

doi:10.1186/1747-1028-8-8
Cite this article as: Miyaoka and Miyajima: **To divide or not to divide: revisiting liver regeneration.** *Cell Division* 2013 **8**:8.

Biochemical and Biophysical Research Communications 435 (2013) 447–453

Contents lists available at SciVerse ScienceDirect

Biochemical and Biophysical Research Communications

journal homepage: www.elsevier.com/locate/ybbrc

Acetylcholine receptors regulate gene expression that is essential for primitive streak formation in murine embryoid bodies

Norie Arima [a,1], Yoshimi Uchida [a,1], Ruoxing Yu [a], Koh Nakayama [b], Hiroshi Nishina [a,*]

[a] Department of Developmental and Regenerative Biology, Medical Research Institute, Tokyo Medical and Dental University, 1-5-45 Yushima, Bunkyo-ku, Tokyo 113-8510, Japan
[b] Oxygen Biology Unit, Frontier Research Laboratory, Medical Research Institute Tokyo Medical and Dental University, Tokyo, Japan

ARTICLE INFO

Article history:
Received 29 April 2013
Available online 10 May 2013

Keywords:
Muscarinic acetylcholine receptor
Primitive streak
Retinoic acid
Cyp26a1
Wnt3
Embryonic stem cell

ABSTRACT

Muscarinic acetylcholine receptors (mAchRs) are critical components of the cholinergic system, which is the key regulator of both the central and peripheral nervous systems in mammals. Interestingly, several components of the cholinergic system, including mAchRs and choline acetyltransferase (ChAT), have recently been found to be expressed in mouse embryonic stem (ES) cells and human placenta. These results raise the intriguing possibility that mAchRs play physiological roles in the regulation of early embryogenesis. Early embryogenesis can be mimicked *in vitro* using an ES cell-based culture system in which the cells form a primitive streak-like structure and efficiently develop into mesodermal progenitors. Here we report that chemical inhibitors specifically targeting mAchRs suppressed the expression of genes essential for primitive streak formation, including *Wnt3*, and thereby blocked mesodermal progenitor differentiation. Interestingly, mAchR inhibitors also reduced the expression of *Cyp26a1*, an enzyme involved in the catabolism of retinoic acid (RA). RA is an important regulator of *Wnt3* signaling. Our study presents evidence indicating that mAchRs influence RA signaling necessary for the induction of the primitive streak. To our knowledge, this is the first report showing that mAchRs have important functions not only in adult mammals but also during early mammalian embryogenesis.

1. Introduction

Muscarinic acetylcholine receptors (mAchRs) are expressed in virtually all organs, tissues and cell types of adult mammals, and play key roles in neuronal systems. In the central nervous system, mAchRs regulate locomotor activity and cognitive functions. In peripheral parasympathetic nervous systems, acetylcholine released by vagal nerve endings stimulates mAchRs, thereby inducing muscle contraction and gland secretions [1]. Intriguingly, recent work has shown that components of the cholinergic system, including mAchRs and enzymes of acetylcholine metabolism, are also expressed in murine embryonic stem (ES) cells [2]. In addition, the enzyme that synthesizes acetylcholine, choline acetyltransferase (ChAT), has been detected in human placenta [3]. These studies suggest that mAchRs play physiological roles during early development as well as at the adult stage. However, the molecular mechanisms by which mAChRs are involved in early embryonic development are unclear.

In mammalian embryos, a single layer of epithelial cells called the epiblast generates the three germ layers – the mesoderm, endoderm and ectoderm – through the primitive streak. The primitive streak induces differentiation of mesoderm and endoderm at the posterior pole of the embryo [4], whereas the anterior epiblast expressing *SRY-box containing gene 2* (*Sox2*) differentiates into neuroectodermal derivatives [5]. Primitive streak formation is regulated by many extracellular signals but particularly by those mediated via the "wingless-related MMTV integration site 3" (Wnt3) pathway [6]. Retinoic acid (RA) also plays a key role in primitive streak formation, and RA abundance in a mammalian embryo is determined by a balance between RA synthesis by retinaldehyde dehydrogenase (RALDH) and RA degradation mediated by CYP26 [7,8].

To investigate the roles of mAchRs in early embryogenesis, we used a murine system in which ES cells derived from the inner cell mass of the blastocyst are induced to aggregate in culture and form an embryoid body (EB) [9]. EB formation mimics early embryogenesis *in vivo*, in that the ES cells can differentiate into the usual three germ layers. In the presence of Wnt3 signaling, a primitive streak-like region is established in EBs that generates mesodermal progenitor cells in this region [10]. In this study, we have used the EB system to demonstrate that mAchRs are required for the expression of genes essential for primitive streak and mesoderm formation.

Abbreviations: ChAT, choline acetyltransferase; DH, dicyclomine hydrochloride; EB, embryoid body; mAchR, muscarinic acetylcholine receptor; RA, retinoic acid.

* Corresponding author. Fax: +81 3 5803 5829.
E-mail address: nishina.dbio@mri.tmd.ac.jp (H. Nishina).

[1] These authors contributed equally to this work.

0006-291X/$ - see front matter © 2013 Elsevier Inc. All rights reserved.
http://dx.doi.org/10.1016/j.bbrc.2013.05.006

2. Materials and methods

2.1. Reagents and antibodies

Aprofene (InterBioScreen Ltd., Bio-0805), dicyclomine hydrochloride (Sigma, D7909), and retinoic acid (Sigma, R2625) were purchased from the indicated suppliers. Antibodies (Abs) recognizing the following proteins were used in this study: β-tubulin III (Tuj-1, Covance, MMS-435P), sarcomeric α-actinin (Abcam, ab9465), GAPDH (Millipore, MAB374), synaptophysin (Invitrogen, 18–0130), and SOX2 (Santa Cruz Biotechnology, sc-17320).

2.2. ES cell culture and differentiation

Embryoid bodies (EBs) were prepared as described previously [11,12]. Briefly, undifferentiated ES cells were dissociated into single-cell suspensions and cultured in hanging drops to induce embryoid body (EB) formation. Initial cell density (on Day 0) was 3000 cells per drop (25 μl) of differentiation medium without LIF. After two days in hanging drop culture in the absence or presence of aprofene (final concentration 10 μM), the resulting EBs were transferred to non-coated culture dishes (Day 2). On Day 6, the EBs were plated in plastic gelatin-coated dishes and cultured until Day 12. Culture medium was changed every 2 days. EBs were left untreated, or treated with 10 μM aprofene or 10 μM DH or 1 pM RA during days 1–6.

2.3. Immunostaining

Immunostaining was performed as described [11,12]. EBs were washed with phosphate-buffered saline (PBS) and fixed in 4% paraformaldehyde (PFA)/0.1% Triton X-100. Fixed EBs were incubated with blocking solution [5% bovine serum albumin (BSA)/PBS/0.1% Triton X-100] for 30 min at room temperature (RT). Blocked EBs were incubated overnight with primary Ab (1:1000 dilution) at 4 °C followed by two washes in PBS/0.1% Triton X-100. Washed EBs were incubated for 1 h at RT with AlexaFluor568- or Cy3-conjugated secondary Ab (1:1000 dilution) plus 8 μM Hoechst 33342. Stained EBs were washed three times in PBS/0.1% Triton X-100.

2.4. Immunoblotting

Immunoblotting was performed as described [13]. ES cells or EBs were homogenized in RIPA buffer [150 mM NaCl, 5 mM ethylenediamine tetra-acetic acid (EDTA), 0.1% Nonidet P-40, 1 mM dithiothreitol (DTT), 0.5% deoxycholic acid, and 50 mM Tris–HCl pH 8.0] containing protease inhibitor mixture tablets. Lysates were clarified by centrifugation for 5 min at 12,000*g*, and protein concentrations of supernatants were equalized using the Pierce BCA Protein Assay Kit (Thermo). Supernatants were fractionated by standard sodium dodecyl sulfate–polyacrylamide gel electrophoresis (SDS–PAGE) and transferred by electroblotting onto polyvinylidene difluoride membranes. Membranes were blocked with 2% nonfat milk or Blocking One (Nacalai Tesque) and incubated overnight at 4 °C with primary antibody. Blots were then incubated with the appropriate secondary antibody and developed with the ECL detection system (Amersham Biosciences).

2.5. Quantitative reverse transcriptase-polymerase chain reaction (qRT-PCR) and reverse transcriptase-polymerase chain reaction (RT-PCR)

qRT-PCR and RT-PCR were performed as described [11–13]. Total RNA extraction was carried out using Tri Reagent (Molecular Research Center) according to the manufacturer's instructions. Total RNA (4 μg) was reverse-transcribed into cDNA using Superscript III RNase H Reverse Transcriptase (Invitrogen) and 500 ng Oligo-d(T) primers. Each quantitative real-time RT-PCR reaction was performed using the Chromo4 real-time detection system (Bio-Rad). For a 20 μl PCR reaction, 10 μl containing cDNA template mixed with the appropriate primers to a final concentration of 200 nM was combined with 10 μl Eva Green (Biotium). The reaction was incubated at 95 °C for 3.5 min, followed by 40 cycles at 95 °C for 20 s, 60 °C for 20 s, and 72 °C for 20 s. PCR primers are listed in Supplementary Table S1.

3. Results

3.1. Inhibition of mAchRs alters gene expression patterns associated with EB differentiation

To investigate the role of mAchRs in early embryogenesis, we used two specific inhibitors of mAchRs, aprofene [14] and dicyclomine hydrochloride (DH) [15], and an *in vitro* ES cell-based system in which ES cells can be induced to efficiently differentiate into mesodermal progenitors through a primitive streak-like structure. These progenitors normally differentiate into cardiomyocytes that soon commence cardiac "beating", but inhibition of this cardiomyogenesis results in the induction of neurogenesis [12]. When we used either mAchR inhibitor to treat differentiating EBs, no "beating" ES cells could be detected upon examination on day 12 (Fig. 1A), indicating that cardiomyocyte differentiation was completely blocked. *In vitro*, both mAchR inhibitors efficiently suppressed the mRNA expression of the cardiac-associated gene *a-cardiac Myosin heavy chain* (*Mhc*) (Fig. 1B). However, mRNA expression of the neuronal lineage gene *Microtubule-associated protein 2* (*Map2*) was increased in these cells (Fig. 1C). Immunostaining of EB outgrowths in culture revealed positive staining for β-tubulin III, a neuron-specific marker (Fig. 1D). The expression in our EB system of mRNAs for mAchRs [*cholinergic receptor, muscarinic* (*Chrm*) *1–5*], as well as *Choline acetyltransferase* (*Chat*), the enzyme that synthesizes acetylcholine, was confirmed by RT-PCR. *Chrm2, 3, 5, and Chat* were detected in both ES cells and EBs (Fig. 1E). *Chrm4* expression was found only in EBs. *Chrm1* was not expressed in either ES cells or EBs. These results suggest that mAchRs promote cardiomyocyte differentiation during murine embryogenesis.

3.2. Inhibition of mAchRs during days 3–4 of EB differentiation decreases cardiomyocyte differentiation

To determine precisely when mAchRs influence ES cell differentiation, we treated EBs with aprofene or DH for various time periods. As shown in Fig. 2A and B, treatment with either aprofene or DH significantly decreased the proportion of EBs containing beating foci (the "beating ratio") only when the inhibitor was applied between days 3–4. Treatment for any other period did not reduce the beating ratio. Next, we measured the mRNA expression and protein levels of cardiomyocyte and neuronal markers by immunoblotting and qRT-PCR. Our immunoblotting analysis indicated that expression of the cardiac-specific protein sarcomeric-actinin was reduced in EBs treated with aprofene during days 3–4 compared to untreated controls, or compared to EBs treated with aprofene for other periods (Fig. 2C). In contrast, the expression of the neuron-specific protein synaptophysin was sharply induced by aprofene treatment during days 3–4 (Fig. 2C). qRT-PCR analysis confirmed that the mRNA expression of the cardiac-specific gene *Mhc* was suppressed by mAchR inhibition during days 3–4 (Fig. 2D), but that mRNA expression of the neuron-specific gene *Map2* was induced by this treatment (Fig. 2E). Thus, the critical

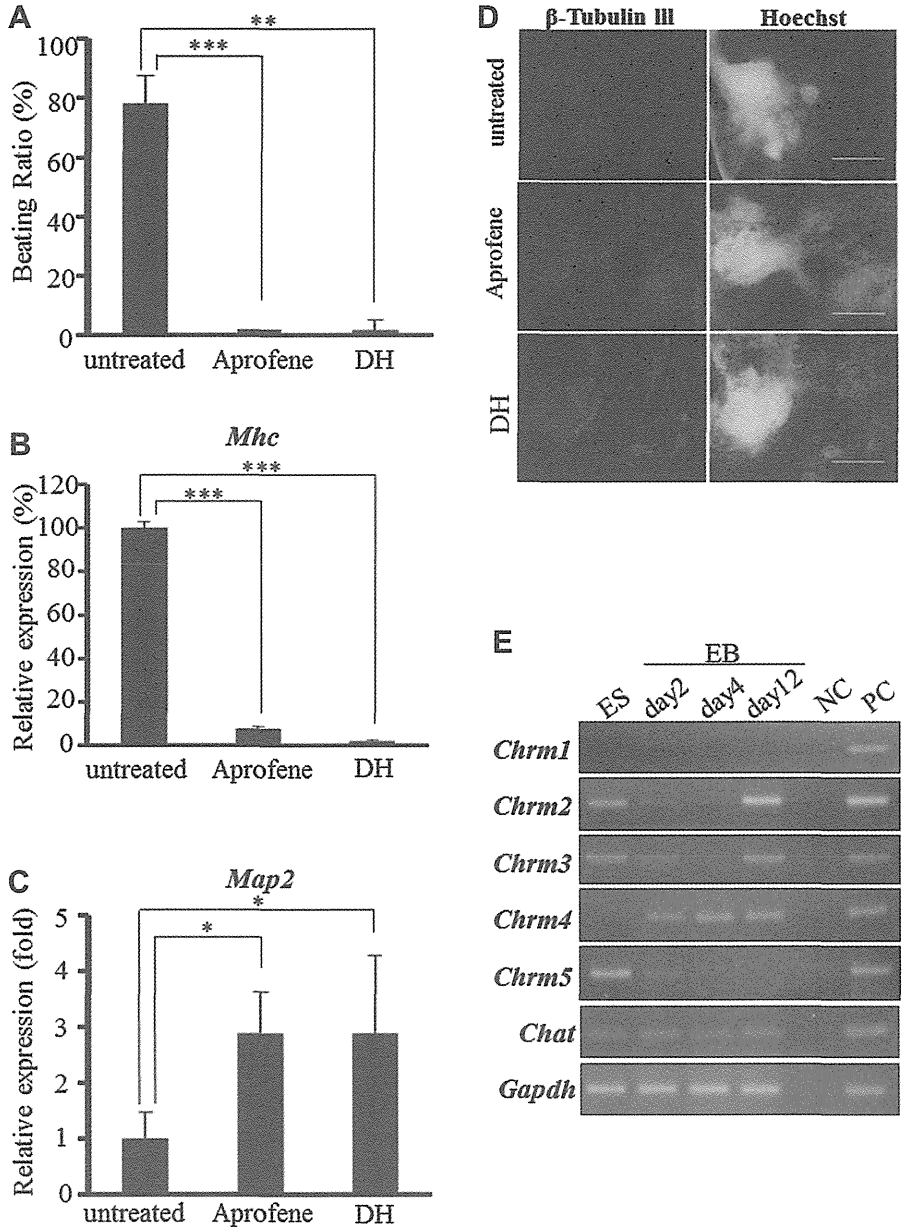

Fig. 1. Effects of mAchR inhibitors on gene expression patterns during EB differentiation. (A) Decreased cardiomyocyte differentiation. EBs were left untreated, or treated with 10 μM aprofene or 10 μM DH during days 1–6, and cultured for a total of 12 days. The number of EBs containing beating foci were counted on day 12. Data are the mean ratio ± SD of EBs with beating foci among total EBs plated, expressed as a percentage. For all figures, results are representative of at least 3 independent trials. (B, C) Decreased cardiac-specific but increased neuron-specific gene expression. mRNA was extracted from the EBs in (A) on day 12 and analyzed by qRT-PCR to detect transcripts of the cardiac-specific gene *Mhc* (B) and the neuron-specific gene *Map2* (C). Data were normalized to *Gapdh* mRNA levels and are expressed as the relative mean ± SD. (D) Increased neural outgrowths. EBs were left untreated, or treated with 10 μM aprofene or 10 μM DH dicyclomine hydrochloride (DH) during days 2–6, and outgrowths in culture were examined on day 12. Neuronal lineage cells within EB outgrowths were detected by immunostaining with anti-β-tubulin III antibody. Nuclear were stained with hoechst 33342. Data are representative of 3 cultures examined per condition. Scale bar, 500 μm. (E) Confirmation of mAchR and ChAT mRNA expression. mRNA was extracted from ES cells and untreated EBs on days 2, 4 and 12, and subjected to RT-PCR analysis to detect *ChrmR1–5* (encoding mAchR1–5) and *ChAT* mRNAs. *Gapdh*, loading control. Negative control (NC): without reverse transcriptase. Positive control (PC): adult mouse brain. $^{*}P < 0.05$, $^{**}P < 0.0001$, $^{***}P < 1 \times 10^{-5}$.

period of mAchR influence on cardiomyogenesis is days 3–4 of EB differentiation.

3.3. Inhibition of mAchRs reduces primitive streak gene expression

The expression of genes essential for mesoderm formation has been previously shown to increase from day 3 and peak at day 4 *in vitro* ES cell-based systems [16,17]. We confirmed this pattern in our system by examining the expression of *T-brachyury* (*T*), a gene required for the generation of mesodermal progenitors. When we treated EBs with aprofene during days 1–4, *T* expression was dramatically decreased (Fig. 3A). In contrast, expression of the neuroectodermal gene *Sox2*, which normally drops to a low level in untreated EBs by day 4, did not decrease in aprofene-treated EBs (Fig. 3B). Immunoblotting analysis confirmed that aprofene treatment blocked the expected reduction in SOX2 protein on day 4 (Fig. 3C). Because these data suggested that primitive streak formation was impaired in aprofene-treated EBs, we examined the mRNA expression of a variety of primitive streak genes, including *Wnt3*, *Wnt3a*, *LIM homeobox protein 1* (*Lhx1*), *Wnt8a*, and *fibroblast*

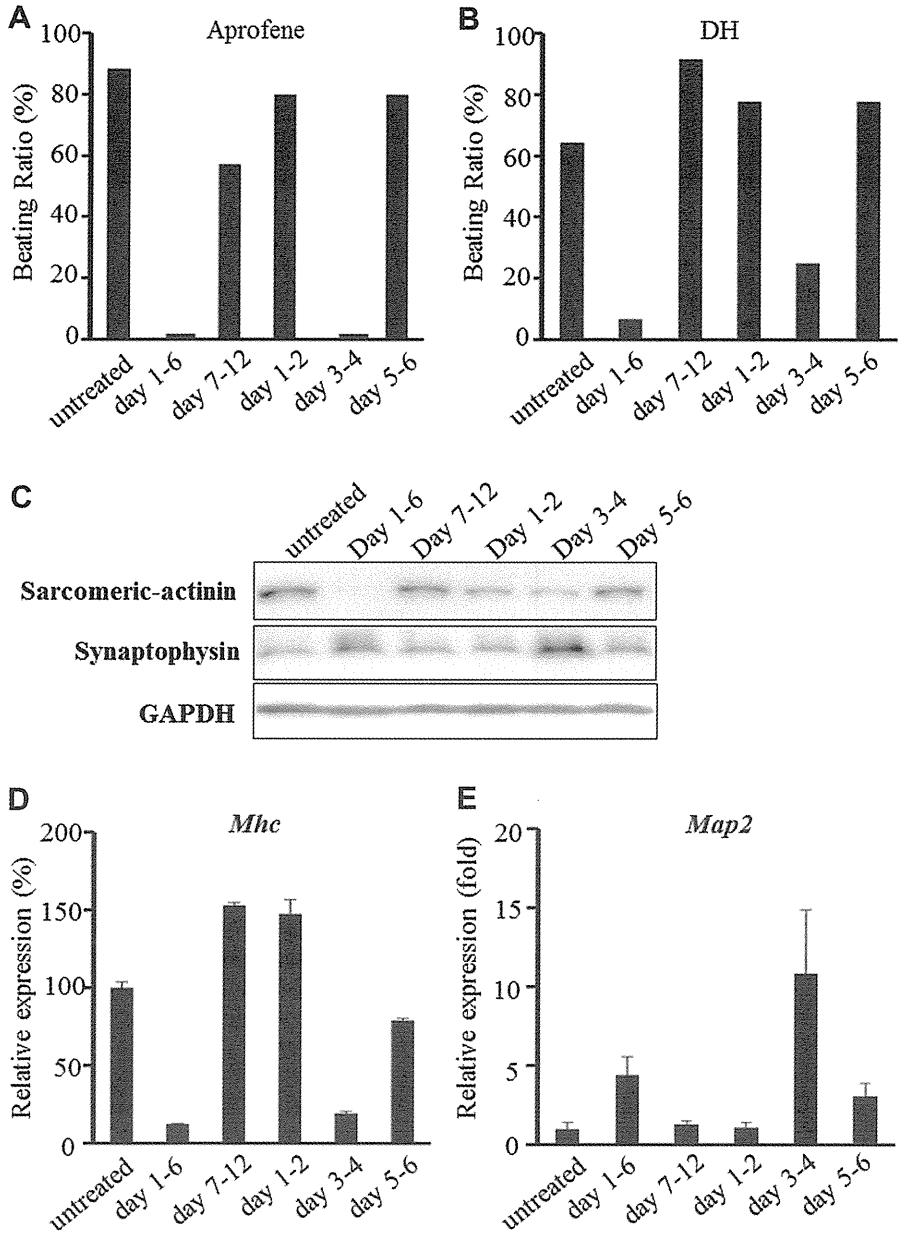

Fig. 2. Inhibition of mAchRs on days 3–4 of EB differentiation decreases cardiomyocyte differentiation. (A, B) Narrow window of mAchR influence. EBs were left untreated or treated with 10 μM aprofene (A) or 10 μM DH (B) for the indicated time periods. On day 12, cardiomyocyte differentiation was determined as for Fig. 1A. (C) Altered lineage-specific proteins. Extracts from the EBs in (A) were analyzed by immunoblotting to detect cardiac-specific sarcomeric α-actinin and neuron-specific synaptophysin. GAPDH, loading control. Results are representative of at least 3 trials. (D, E) Altered lineage-specific mRNAs. Extracts from the EBs in (A) were subjected to qRT-PCR to detect mRNA expression levels of the cardiac-specific gene *Mhc* (D) or the neuron-specific gene *Map2* (E). Results were analyzed as for Fig. 1B.

growth factor 8 (*Fgf8*). Transcript levels of all of these genes were significantly reduced in aprofene-treated EBs on day 4 compared to untreated EBs (Fig. 3D). These data indicate that mAchRs regulate gene expression associated with primitive streak formation and the subsequent differentiation of mesodermal progenitors.

3.4. mAchRs influence primitive streak gene expression through effects on RA

As noted above, RA signaling plays a key regulatory role in primitive streak formation by controlling Wnt3 signaling [8]. We therefore examined the expression of primitive streak and mesodermal genes in EBs treated with RA during days 1–4. We found that mRNA levels of *Wnt3*, *Wnt3a*, *Lhx1* and *T* were all significantly decreased in RA-treated EBs (Fig. 4A). To investigate whether the effects of mAchRs on EB differentiation were due to modulation of RA signaling, we measured the mRNA expression of genes encoding enzymes involved in RA metabolism. Expression of *aldhyde dehydrogenase 1* (*Aldh1*), an enzyme required for RA synthesis, was comparable between untreated and aprofene-treated EBs (Fig. 4B). However, mRNA levels of *cytochrome P450, family 26, subfamily a, polypeptide 1*(*Cyp26a1*), which is critical for RA catabolism, were markedly decreased by aprofene treatment (Fig. 4C). These findings indicate that mAchRs support primitive streak formation leading to mesodermal progenitor generation and cardiomyocyte differentiation by increasing *Cyp26a1* expression, thereby promoting RA degradation and allowing Wnt3 signaling to proceed.

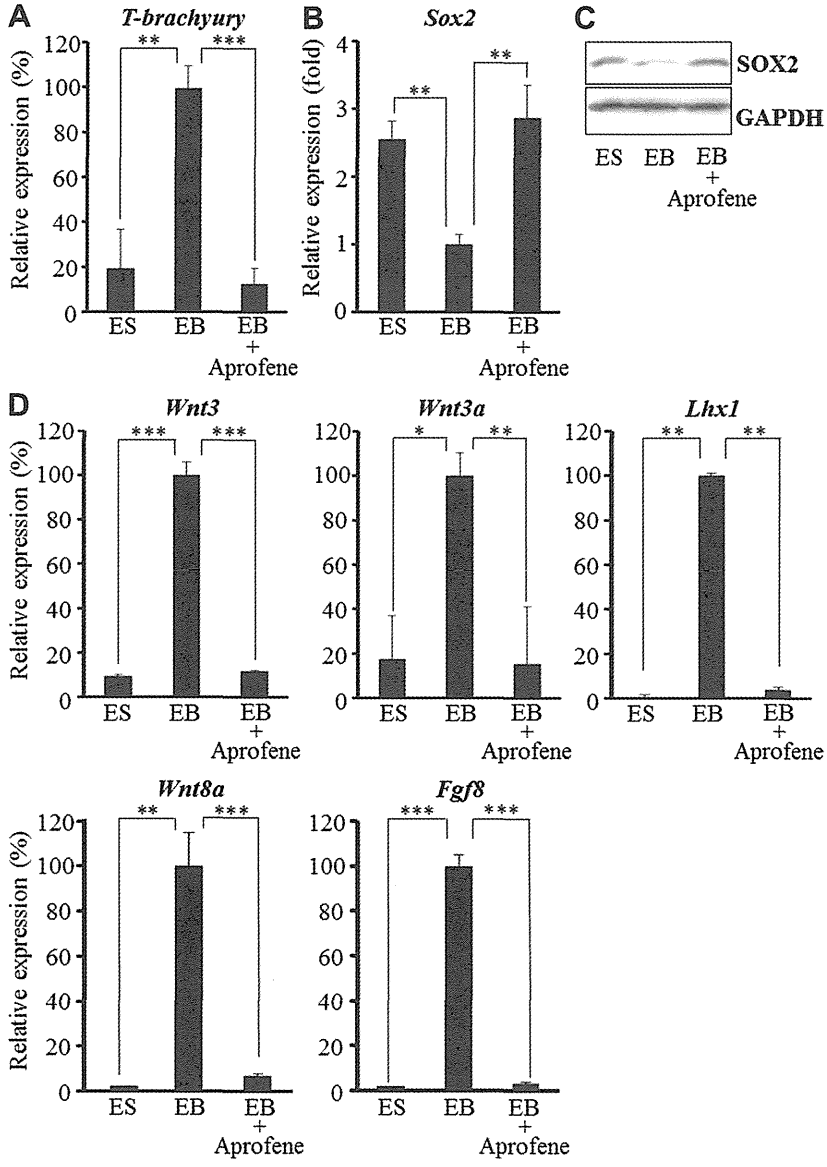

Fig. 3. Inhibition of mAchRs reduces primitive streak gene expression. (A) Decreased mesodermal gene expression. EBs were left untreated or treated with 10 μM aprofene during days 1–4. mRNA was extracted from control ES cells, or untreated or treated EBs on day 4, and analyzed by qRT-PCR to detect mRNA levels of *T-brachyury* (*T*). (B, C) Resistant *Sox2* expression. The extracts in (A) were analyzed by qRT-PCR (B) or immunoblotting (C) to detect *Sox2* mRNA or protein, respectively, as for Fig. 2B and C. (D) Decreased expression of primitive streak genes. The extracts in (A) were analyzed by qRT-PCR to detect mRNA levels of the indicated primitive streak genes. For A, B and D, results were analyzed as for Fig. 1B. $^{*}P < 0.05$, $^{**}P < 0.0001$, $^{***}P < 1 \times 10^{-5}$.

4. Discussion

In this study, we investigated the function of mAchRs during early murine embryogenesis. As depicted in Fig. 4D, our data suggest a model in which mAchRs promote the expression of *Cyp26a1*, a gene encoding an enzyme involved in RA catabolism. This moderation of RA concentration then enables Wnt3 to induce primitive streak genes, which in turn promote the differentiation of ES cells into mesodermal progenitors and ultimately cardiomyocytes, at the expense of neuronal lineages.

In early embryos, RA abundance is mainly determined by degradation mediated by CYP26 [18]. Previous studies have demonstrated that *Cyp26a1* is highly expressed during early embryonic patterning, and that depletion of maternal RA by embryonic CYP26 is required for proper primitive streak formation. Accordingly, *Cyp26a1/b1/c1* knockout mice show abnormalities in primitive streak formation. Our data shown in Fig. 4 are consistent with these reports.

Our results also show that mAchR inhibition increased the expression of ectodermal genes and promoted neurogenesis (Figs. 1 and 3). Knockout mice deficient for primitive streak genes, such as *Wnt3*$^{-/-}$ mice, exhibit similar phenotypes of decreased mesoderm formation and an expanded ectodermal region [19]. Taken together, these observations suggest that inhibition of primitive streak formation may enhance neuroectodermal differentiation *in vivo* and *in vitro*.

There are five mAchR subtypes, mAchR1–5. It has been previously reported that neither single knockout mice for any of these five genes, nor various double knockout mutants (mAchR1$^{-/-}$ and mAchR3$^{-/-}$, mAchR1$^{-/-}$ and mAchR4$^{-/-}$, mAchR1$^{-/-}$ and mAchR5$^{-/-}$, mAchR2$^{-/-}$ and mAchR3$^{-/-}$, mAchR2$^{-/-}$ and mAchR4$^{-/-}$), show severe developmental abnormalities [20].

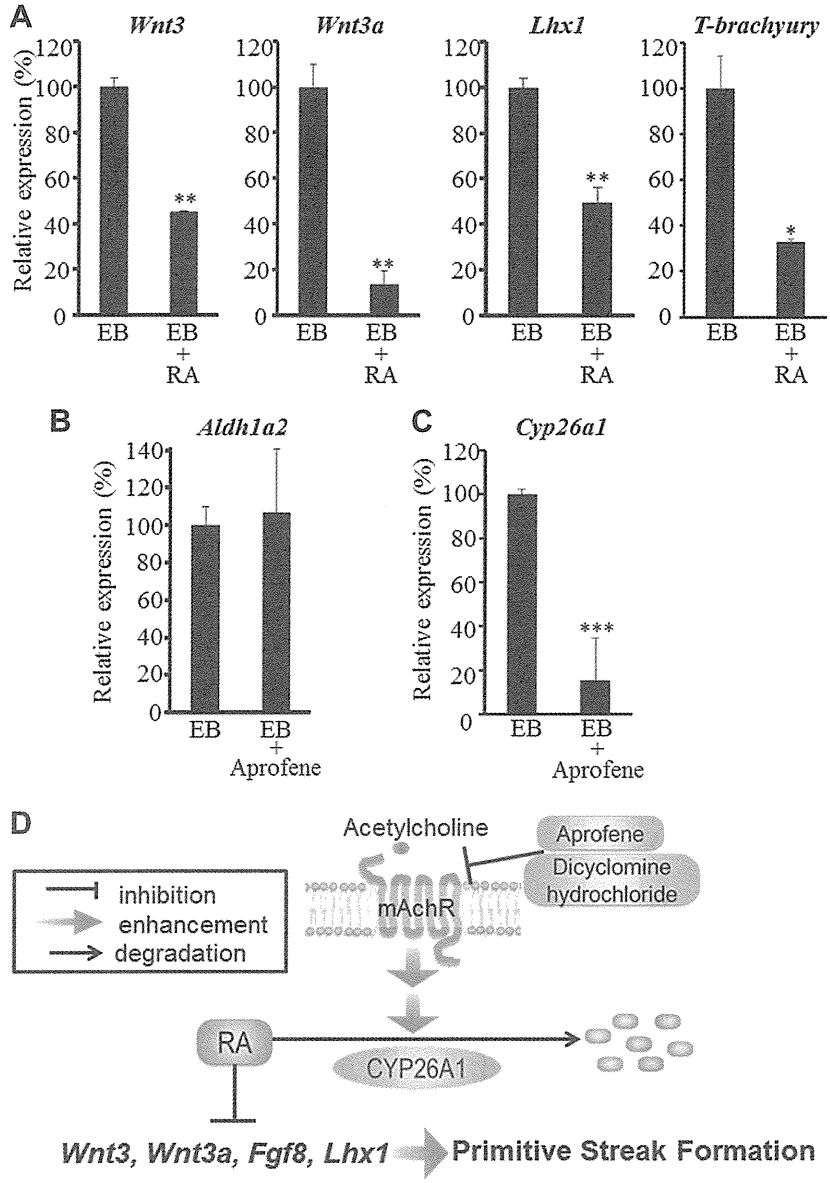

Fig. 4. mAchRs influence primitive streak gene expression through effects on RA. (A) RA reduces primitive streak gene expression. EBs were left untreated or treated with 1 pM RA during days 1–4 from day 1 and extracts were analyzed by qRT-PCR on day 4 to detect mRNA levels of the indicated primitive streak genes. Data were analyzed as for Fig. 1B. (B, C) mAchR inhibition reduces *Cyp26a1* expression. EBs were left untreated or treated with 10 μM aprofene during days 1–4 from day 1 and extracts were analyzed by qRT-PCR on day 4 to detect mRNA levels of the RA anabolic enzyme Aldh1a2 (B) and the RA catabolic enzyme Cyp26a1 (C). Data were analyzed as for Fig. 1B. (D) A model depicting a putative mechanism by which mAchRs can influence primitive streak formation. RA normally inhibits the expression of a variety of primitive streak genes, including Wnt3. RA abundance is controlled by degradation mediated by the catabolic enzyme Cyp26A1, whose expression is enhanced by mAchR activity. $^{*}P < 0.05$, $^{**}P < 0.0001$, $^{***}P < 1 \times 10^{-5}$.

However, these normal phenotypes may have been due to the redundancy of mAchR genes. We have shown, using two chemical inhibitors that specifically block five mAchRs [21–23], that embryonic development patterns are clearly altered in the absence of mAchR function. Thus, although the mechanism by which mAchRs control *Cyp26a1* expression has yet to be clarified, our work has revealed a novel physiological function for mAchRs in influencing gene expression required for embryogenesis.

Acknowledgments

This work was supported in part by research grants from the Ministry of Education, Culture, Sports, Science and Technology of Japan, the Ministry of Health, Labour and Welfare of Japan, and the Japan Society for the Promotion of Science.

Appendix A. Supplementary data

Supplementary data associated with this article can be found, in the online version, at http://dx.doi.org/10.1016/j.bbrc.2013.05.006.

References

[1] M.P. Caulfield, N.J. Birdsall, International union of pharmacology. XVII. Classification of muscarinic acetylcholine receptors, Pharmacol. Rev. 50 (1998) 279–290.

[2] L.E. Paraoanu, G. Steinert, A. Koehler, I. Wessler, P.G. Layer, Expression and possible functions of the cholinergic system in a murine embryonic stem cell line, Life Sci. 80 (2007) 2375–2379.

[3] I. Wessler, R. Michel-Schmidt, C. Brochhausen, C.J. Kirkpatrick, Subcellular distribution of choline acetyltransferase by immunogold electron microscopy in non-neuronal cells: placenta, airways and murine embryonic stem cells, Life Sci. 91 (2012) 977–980.

[4] N. Ramkumar, K.V. Anderson, SnapShot: mouse primitive streak, Cell 146 (2011) 488.
[5] H.B. Wood, V. Episkopou, Comparative expression of the mouse Sox1, Sox2 and Sox3 genes from pre-gastrulation to early somite stages, Mech. Dev. 86 (1999) 197–201.
[6] P. Liu, M. Wakamiya, M.J. Shea, U. Albrecht, R.R. Behringer, A. Bradley, Requirement for Wnt3 in vertebrate axis formation, Nat. Genet. 22 (1999) 361–365.
[7] R.K. Kam, Y. Deng, Y. Chen, H. Zhao, Retinoic acid synthesis and functions in early embryonic development, Cell Biosci. 2 (2012) 11.
[8] N. Engberg, M. Kahn, D.R. Petersen, M. Hansson, P. Serup, Retinoic acid synthesis promotes development of neural progenitors from mouse embryonic stem cells by suppressing endogenous, Wnt-dependent nodal signaling, Stem Cells 28 (2010) 1498–1509.
[9] T.C. Doetschman, H. Eistetter, M. Katz, W. Schmidt, R. Kemler, The *in vitro* development of blastocyst-derived embryonic stem cell lines: formation of visceral yolk sac, blood islands and myocardium, J. Embryol. Exp. Morphol. 87 (1985) 27–45.
[10] D. ten Berge, W. Koole, C. Fuerer, M. Fish, E. Eroglu, R. Nusse, Wnt signaling mediates self-organization and axis formation in embryoid bodies, Cell Stem Cell 3 (2008) 508–518.
[11] N. Shimizu, H. Watanabe, J. Kubota, J. Wu, R. Saito, T. Yokoi, T. Era, T. Iwatsubo, T. Watanabe, S. Nishina, N. Azuma, T. Katada, H. Nishina, Pa6–5a promotes neuronal differentiation of murine embryonic stem cells, Biol. Pharm. Bull. 32 (2009) 999–1003.
[12] J. Wu, J. Kubota, J. Hirayama, Y. Nagai, S. Nishina, T. Yokoi, Y. Asaoka, J. Seo, N. Shimizu, H. Kajiho, T. Watanabe, N. Azuma, T. Katada, H. Nishina, P38 mitogen-activated protein kinase controls a switch between cardiomyocyte and neuronal commitment of murine embryonic stem cells by activating myocyte enhancer factor 2C-dependent bone morphogenetic protein 2 transcription, Stem Cells Dev. 19 (2010) 1723–1734.
[13] Y. Uchida, T. Osaki, T. Yamasaki, T. Shimomura, S. Hata, K. Horikawa, S. Shibata, T. Todo, J. Hirayama, H. Nishina, Involvement of stress kinase mitogen-activated protein kinase kinase 7 in regulation of mammalian circadian clock, J. Biol. Chem. 287 (2012) 8318–8326.
[14] H. Leader, A.D. Wolfe, P.K. Chiang, R.K. Gordon, Pyridophens: binary pyridostigmine-aprophen prodrugs with differential inhibition of acetylcholinesterase, butyrylcholinesterase, and muscarinic receptors, J. Med. Chem. 45 (2002) 902–910.
[15] J.W. Downie, D.A. Twiddy, S.A. Awad, Antimuscarinic and noncompetitive antagonist properties of dicyclomine hydrochloride in isolated human and rabbit bladder muscle, J. Pharmacol. Exp. Ther. 201 (1977) 662–668.
[16] A.L. Evans, T. Faial, M.J. Gilchrist, T. Down, L. Vallier, R.A. Pedersen, F.C. Wardle, J.C. Smith, Genomic targets of brachyury (T) in differentiating mouse embryonic stem cells, PLoS ONE 7 (2012) e33346.
[17] D.G. Wilkinson, S. Bhatt, B.G. Herrmann, Expression pattern of the mouse T gene and its role in mesoderm formation, Nature 343 (1990) 657–659.
[18] M. Uehara, K. Yashiro, K. Takaoka, M. Yamamoto, H. Hamada, Removal of maternal retinoic acid by embryonic CYP26 is required for correct nodal expression during early embryonic patterning, Gene. Dev. 23 (2009) 1689–1698.
[19] P.P. Tam, D.A. Loebel, Gene function in mouse embryogenesis: get set for gastrulation, Nat. Rev. Genet. 8 (2007) 368–381.
[20] J. Wess, Muscarinic acetylcholine receptor knockout mice: novel phenotypes and clinical implications, Annu. Rev. Pharmacol. Toxicol. 44 (2004) 423–450.
[21] H. Leader, R.K. Gordon, J. Baumgold, V.L. Boyd, A.H. Newman, R.M. Smejkal, P.K. Chiang, Muscarinic receptor subtype specificity of N, N-dialkylamino)alkyl 2-cyclohexyl-2-phenylpropionates: cylexphenes (cyclohexyl-substituted aprophen analogues, J. Med. Chem. 35 (1992) 1290–1295.
[22] N.J. Buckley, T.I. Bonner, C.M. Buckley, M.R. Brann, Antagonist binding properties of five cloned muscarinic receptors expressed in CHO-K1 cells, Mol. Pharmacol. 35 (1989) 469–476.
[23] M. Eltze, M. Galvan, Involvement of muscarinic M2 and M3, but not of M1 and M4 receptors in vagally stimulated contractions of rabbit bronchus/trachea, Pulm. Pharmacol. 7 (1994) 109–120.

Developmental Cell
Short Article

Control of the Hippo Pathway by Set7-Dependent Methylation of Yap

Menno J. Oudhoff,[1] Spencer A. Freeman,[2] Amber L. Couzens,[5] Frann Antignano,[1] Ekaterina Kuznetsova,[6] Paul H. Min,[1] Jeffrey P. Northrop,[1] Bernhard Lehnertz,[1] Dalia Barsyte-Lovejoy,[6] Masoud Vedadi,[6] Cheryl H. Arrowsmith,[6,7,8] Hiroshi Nishina,[10] Michael R. Gold,[2] Fabio M.V. Rossi,[1,3] Anne-Claude Gingras,[5,9] and Colby Zaph[1,4,*]

[1]The Biomedical Research Centre
[2]Department of Microbiology and Immunology
[3]Department of Medical Genetics
[4]Department of Pathology and Laboratory Medicine
University of British Columbia, Vancouver, BC V6T 1Z3, Canada
[5]Lunenfeld-Tanenbaum Research Institute, Mount Sinai Hospital
[6]The Structural Genomics Consortium
[7]Princess Margaret Cancer Centre
[8]Department of Medical Biophysics
[9]Department of Molecular Genetics
University of Toronto, Toronto, ON M5G 1L7, Canada
[10]Department of Developmental and Regenerative Biology, Medical Research Institute, Tokyo Medical and Dental University, Tokyo 113-8510, Japan
*Correspondence: colby@brc.ubc.ca
http://dx.doi.org/10.1016/j.devcel.2013.05.025

SUMMARY

Methylation of nonhistone proteins is emerging as a regulatory mechanism to control protein function. Set7 (*Setd7*) is a SET-domain-containing lysine methyltransferase that methylates and alters function of a variety of proteins in vitro, but the in vivo relevance has not been established. We found that Set7 is a modifier of the Hippo pathway. Mice that lack Set7 have a larger progenitor compartment in the intestine, coinciding with increased expression of Yes-associated protein (Yap) target genes. Mechanistically, monomethylation of lysine 494 of Yap is critical for cytoplasmic retention. These results identify a methylation-dependent checkpoint in the Hippo pathway.

INTRODUCTION

The site-specific methylation of histone lysine residues by lysine methyltransferases (KMTs) has been shown to regulate gene expression by modulating chromatin structure to either repress or activate genes at specific loci (Jenuwein and Allis, 2001). More recently, lysine methylation of nonhistone proteins has emerged as a novel regulatory mechanism to control protein function, primarily by affecting stability (Estève et al., 2009; Huang and Berger, 2008; Su and Tarakhovsky, 2006). However, the in vivo relevance of this posttranslational modification remains unknown.

Set7 is a KMT that was initially identified as a monomethylase of histone H3 lysine 4 (H3K4) in vitro (Wang et al., 2001). However, because Set7 is unable to methylate nucleosomes at H3K4 (Chuikov et al., 2004) and *Setd7*$^{-/-}$ mouse embryonic fibroblasts (MEFs) have normal levels of H3K4 methylation (Lehnertz et al., 2011), it is more likely that the primary role for Set7 is methylation of nonhistone substrates (Pradhan et al., 2009). Indeed, Set7 has been shown to methylate and alter function of a wide variety of proteins including Dnmt1, Taf10, p53, Stat3, and NF-κB in vitro (Chuikov et al., 2004; Ea and Baltimore, 2009; Estève et al., 2009; Kouskouti et al., 2004; Kurash et al., 2008; Yang et al., 2009, 2010a, 2010b). However, the in vivo relevance of Set7-dependent methylation has not been established. In fact, a role for Set7 in alteration of p53 function in vivo has recently been refuted (Campaner et al., 2011; Lehnertz et al., 2011), which is in agreement with a study demonstrating that mutation of the lysine residues potentially methylated by Set7 in p53 did not dramatically alter its function (Krummel et al., 2005). Thus, the physiological role for Set7 remains unknown.

The Hippo pathway is an evolutionarily conserved signaling pathway that regulates organ size and function (Cai et al., 2010; Camargo et al., 2007; Dong et al., 2007; Heallen et al., 2011; Schlegelmilch et al., 2011). Canonical activation of the Hippo pathway is initiated by cell-cell contact, cell polarity, and mechanical cues, which through a kinase cascade ultimately leads to the phosphorylation and subsequent cytosolic sequestration and/or degradation of the Hippo pathway transducers Yes-associated protein (Yap) and transcriptional coactivator with PDZ binding motif (Taz) (Kanai et al., 2000). Yap/Taz function as transcriptional coactivators of proliferation and antiapoptosis genes by interacting with transcription factors including the canonical *Drosophila* Scalloped homologs Tead1/4 (Zhao et al., 2008). As dysregulation of Yap/Taz is associated with several types of cancer such as breast, liver, and colon (Cordenonsi et al., 2011; Pan, 2010; Zhou et al., 2011), a better understanding of the molecular pathways controlling the Hippo pathway will be critical in the development of novel Hippo pathway-specific therapeutics. Using cells and mice genetically

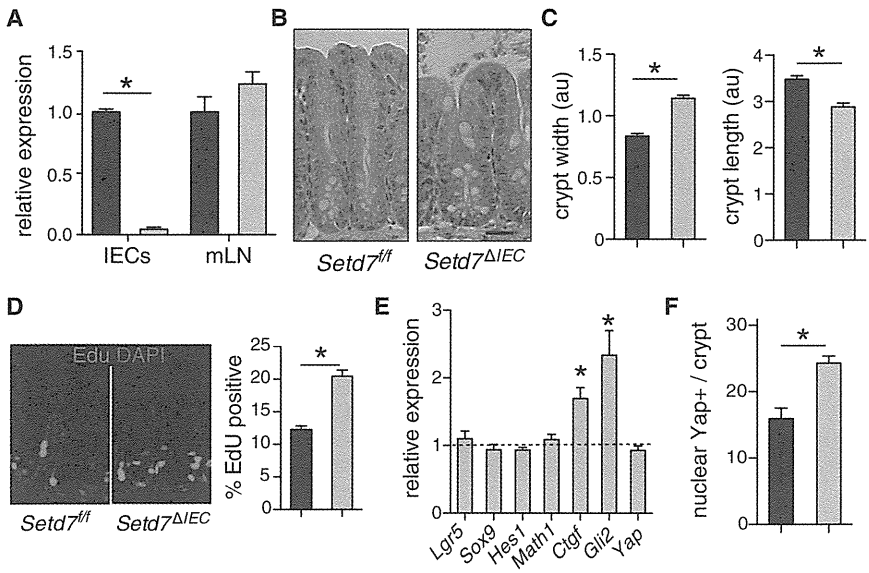

Figure 1. IEC-Intrinsic Expression of Set7 Controls Intestinal Homeostasis

(A) *Setd7*$^{f/f}$ (black bars) and *Setd7*$^{\Delta IEC}$ (gray bars) IECs and mesenteric lymph nodes (mLN) were isolated from *Setd7*$^{f/f}$ and *Setd7*$^{\Delta IEC}$ mice. *Setd7* expression, relative to that in *Setd7*$^{f/f}$ mice, was assessed by qPCR.

(B) H&E stained section of cecal tissue. Bar, 25 μm.

(C) Quantification of crypt width and length (50 crypts per mouse, five mice per group).

(D) Representative cecal section stained for EdU and DAPI. Frequency of EdU-positive cells per crypt is shown in graph (40 crypts per mouse from five mice).

(E) Expression of indicated genes in IECs isolated from naive *Setd7*$^{f/f}$ and *Setd7*$^{\Delta IEC}$ mice was determined by qPCR. Expression is relative to *Setd7*$^{f/f}$ IECs using actin as housekeeping gene.

(F) Cecal sections were analyzed by immunofluorescent staining for Yap. The number of nuclei per crypt that exhibited characteristic speckled nuclear localization of Yap is shown (50 crypts per mouse from five mice per group). Data are presented as mean ± SEM (n = 5–10 mice per genotype).

au, arbitrary units. *p < 0.05. See also Figure S1.

deficient in Set7, we demonstrate that Set7 is a central component of the Hippo pathway through the regulation of Yap localization. We show that Yap and Set7 interact, that Yap is monomethylated at K494, and that a mutated Yap (Yap^{K494R}) is not cytoplasmically retained. Taken together, our results identify a methylation-dependent checkpoint in the Hippo pathway that may act as a therapeutic target to modulate this pathway.

RESULTS AND DISCUSSION

To directly assess the cell autonomous role of Set7 in vivo, we generated intestinal epithelial cell (IEC)-specific Set7-deficient mice (*Setd7*$^{\Delta IEC}$ mice) by crossing mice in which exon 2 was flanked with loxP sites (*Setd7*$^{f/f}$ mice) with mice expressing the Cre recombinase under the control of the IEC-specific *Villin* promoter (el Marjou et al., 2004; Lehnertz et al., 2011). *Setd7*$^{\Delta IEC}$ mice lack *Setd7* expression specifically in IECs (Figure 1A) and display no overt phenotypes. However, examination of the intestines of *Setd7*$^{\Delta IEC}$ mice revealed differences in the intestinal architecture compared to that of control *Setd7*$^{f/f}$ mice. Intestinal crypts from *Setd7*$^{\Delta IEC}$ mice were shorter and wider than those of *Setd7*$^{f/f}$ mice (Figures 1B and 1C). We also observed an increased frequency of proliferating cells per crypt in *Setd7*$^{\Delta IEC}$ mice (Figure 1D), as measured by examining cellular uptake of EdU 2 hr following injection. IEC proliferation and differentiation are tightly regulated processes controlled by the Wnt, Notch, and Hippo signaling pathways (Cai et al., 2010; Camargo et al., 2007; van der Flier and Clevers, 2009). We isolated IECs from colons of naive *Setd7*$^{f/f}$ and *Setd7*$^{\Delta IEC}$ mice and measured gene expression of direct and indirect target genes of the different pathways. Wnt (*Lgr5* and *Sox9*) and Notch (*Hes1* and *Math1*) target genes were not differentially expressed in IECs isolated from naive *Setd7*$^{\Delta IEC}$ mice compared to *Setd7*$^{f/f}$ mice (Figure 1E). In contrast, Hippo pathway-associated genes *Ctgf* and *Gli2* were expressed at significantly higher levels in IECs isolated from *Setd7*$^{\Delta IEC}$ mice (Figure 1E), suggesting a cell-intrinsic role for Set7 in regulating Hippo pathway-associated genes.

In wild-type mice, protein expression of the Hippo transducer Yap is only observed in the nuclei of cells at the base of the intestinal crypt and is associated with intestinal stem cells and transit-amplifying progenitor cells (Cai et al., 2010; Camargo et al., 2007). Consistent with increased expression of Yap target genes in IECs from *Setd7*$^{\Delta IEC}$ mice, we observed significantly increased numbers of Yap-positive nuclei per crypt in *Setd7*$^{\Delta IEC}$ mice compared to *Setd7*$^{f/f}$ mice, with differences being most notable in the upper half of the crypt (Figure 1F; Figure S1 available online). From these data, we conclude that IEC-intrinsic expression of Set7 is required to regulate the size of the proliferative progenitor compartment, potentially through regulation of the Hippo pathway. Of note, a previous study has shown that mice with an IEC-intrinsic deletion of the upstream Hippo pathway adaptor protein Salvador1/WW45 (*Sav1*) also had wider and shorter crypts with more proliferative progenitors (Cai et al., 2010).

To directly test whether Set7 was directly involved in regulation of the Hippo pathway, we studied the well-described Hippo-pathway-dependent process, cell-cell contact-mediated growth inhibition (Zhao et al., 2007). We used immortalized MEFs derived from *Setd7*$^{-/-}$ and *Setd7*$^{+/+}$ mice (Lehnertz et al., 2011). Although no difference in proliferation was detected in the first 48 hr after seeding, once cells reached confluence, *Setd7*$^{-/-}$ MEFs were less susceptible to contact inhibition of proliferation than *Setd7*$^{+/+}$ MEFs as indicated by increasing cell number over time (Figure 2A). Although we failed to detect any differences in expression of the canonical Yap target genes *Ctgf* and *Cdc20* in low-density *Setd7*$^{+/+}$ or *Setd7*$^{-/-}$ MEFs, we observed significantly increased expression of *Ctgf* and *Cdc20* in high-density *Setd7*$^{-/-}$ MEFs compared to *Setd7*$^{+/+}$ MEFs (Figure 2B). Furthermore, *Setd7* expression was not affected by cell density and *Yap* expression was similar in *Setd7*$^{+/+}$ or

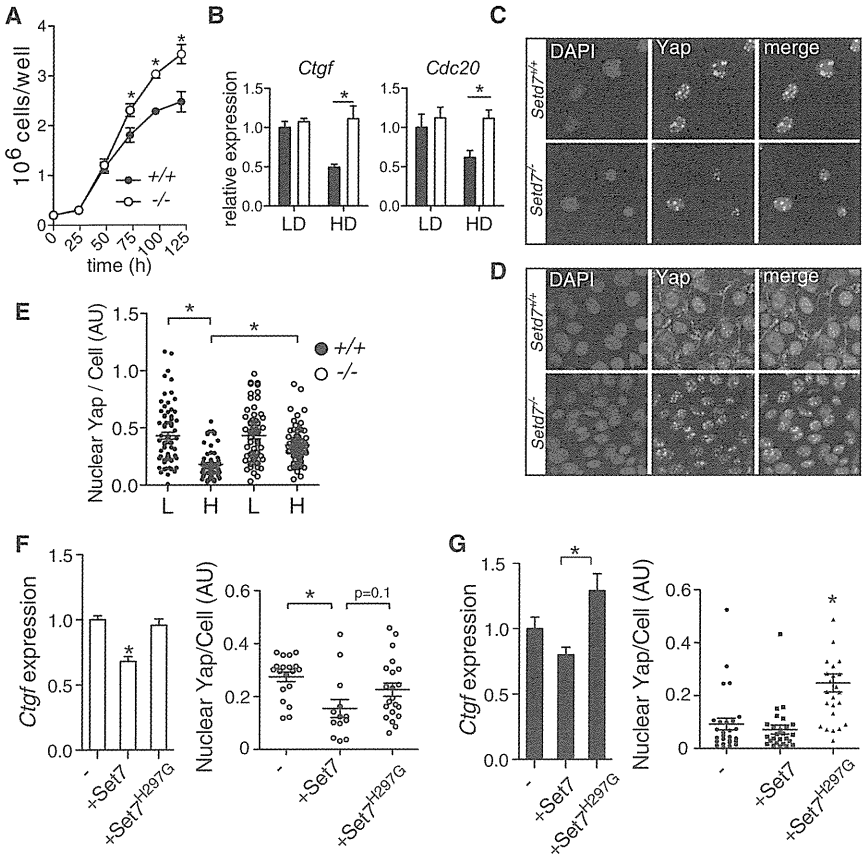

Figure 2. Set7 Regulates Cell-Cell Contact-Mediated Growth Inhibition, and Set7 Methyltransferase Activity Is Required for Yap Localization and Function

(A) *Setd7*$^{+/+}$ (closed circles) and *Setd7*$^{-/-}$ (open circles) MEFs were plated at 2 × 10^5 cells per well, and cell numbers were counted at various time points after plating.

(B) Expression of Yap-dependent genes in low-density (LD) and high-density (HD) *Setd7*$^{+/+}$ (closed bars) and *Setd7*$^{-/-}$ (open bars) MEFs was determined by qPCR. Expression is relative to *Setd7*$^{+/+}$ using actin as housekeeping gene.

(C and D) Yap localization in (C) low-density and (D) high-density *Setd7*$^{+/+}$ and *Setd7*$^{-/-}$ MEFs was determined by immunofluorescent staining.

(E) Nuclear Yap was quantified for individual nuclei of *Setd7*$^{+/+}$ (closed circles) and *Setd7*$^{-/-}$ (open circles) MEFs. L, low-density cultures; H, high-density cultures.

(F) *Setd7*$^{-/-}$ MEFs were transfected with plasmids expressing either Set7 or methyltransferase-deficient Set7^{H297G} and expression of *Ctgf* and Yap localization was determined.

(G) *Setd7*$^{+/+}$ MEFs were transfected with plasmids expressing either Set7 or methyltransferase-deficient Set7^{H297G} and expression of *Ctgf* and Yap localization was determined. Data are mean ± SEM and are representative of two to four independent experiments.

AU, arbitrary units. *p < 0.05. See also Figure S2.

Setd7$^{-/-}$ MEFs at low or high density (Figure S2A). This suggests that Set7 is required for downregulation of Yap-dependent genes in contact-inhibited MEFs.

Yap activity is regulated by cytoplasmic retention and proteasomal degradation, both of which are regulated by phosphorylation (Zhao et al., 2010; Zhao et al., 2007). In low-density cultures, Yap was localized in the nucleus in both *Setd7*$^{+/+}$ and *Setd7*$^{-/-}$ MEFs (Figures 2C and 2E). Consistent with previous studies (Schlegelmilch et al., 2011; Zhao et al., 2007), we observed translocation of Yap to the cytosol and cytoplasmic membrane in high-density cultures of *Setd7*$^{+/+}$ MEFs (Figures 2D and 2E). Strikingly, in high-density *Setd7*$^{-/-}$ MEFs, Yap remained primarily in the nucleus (Figures 2D and 2E), consistent with the increased expression of Yap-dependent genes. Thus, these results demonstrate that Set7 is required for the correct subcellular localization of Yap following cell-cell contact.

Since KMTs can have methyltransferase-independent functions (Lehnertz et al., 2010; Purcell et al., 2011), we next examined whether Yap regulation by Set7 was methyltransferase dependent. We transfected *Setd7*$^{+/+}$ and *Setd7*$^{-/-}$ MEFs with wild-type Set7 or a mutant form of Set7 with a point mutation of residue 297 histidine to a glycine (Set7^{H297G}) that has been shown to inactivate the methyltransferase activity (Nishioka et al., 2002; Tao et al., 2011), and we measured *Ctgf* expression and nuclear Yap. In *Setd7*$^{-/-}$ MEFs, we were able to recover both *Ctgf* gene expression and loss of nuclear Yap (Figure 2F) with Set7 but not Set7^{H297G}, indicating that the methyltransferase activity of Set7 is required for the cytoplasmic retention of Yap and subsequent regulation of target genes. As part of our control experiments, we also transfected the plasmids into *Setd7*$^{+/+}$ MEFs. Strikingly, we found that Set7^{H297G} acts as a dominant negative, as the introduction of this construct in *Setd7*$^{+/+}$ MEFs resulted in increased *Ctgf* expression and enhanced nuclear Yap (Figure 2G). Thus, the methyltransferase activity of Set7 is a critical regulatory mechanism that controls the Hippo pathway through the subcellular localization of Yap.

Following phosphorylation of Yap, two distinct processes—cytoplasmic retention and ubiquitin-mediated degradation—are initiated (Zhao et al., 2010). Although we did not detect cytoplasmic Yap in high-density *Setd7*$^{-/-}$ MEFs by immunofluorescence, we failed to observe a difference in the levels of S127-phosphorylated Yap in *Setd7*$^{+/+}$ and *Setd7*$^{-/-}$ MEFs (Figure 3A), demonstrating that, in the absence of Set7, Yap can exit the nucleus and be phosphorylated but that cytoplasmic retention is impaired. We next tested if degradation of Yap was impaired. To test this, we seeded equal numbers of *Setd7*$^{+/+}$ and *Setd7*$^{-/-}$ MEFs cells at low and high densities by varying the size of the culture dish. Twenty-four hours later, we observed similar density-induced degradation of Yap (Figure 3B), demonstrating that the degradation pathway was not impaired in the absence of Set7. Furthermore, when we left high-density cultures to overgrow for an additional 48 hr, we observed reduced total Yap levels in *Setd7*$^{-/-}$ MEFs compared to *Setd7*$^{+/+}$ MEFs (Figure 3C), suggesting that cytoplasmic retention and not degradation was impaired in the absence of Set7. Consistent with this, confocal microscopy of the overgrown (hyperconfluent) cells

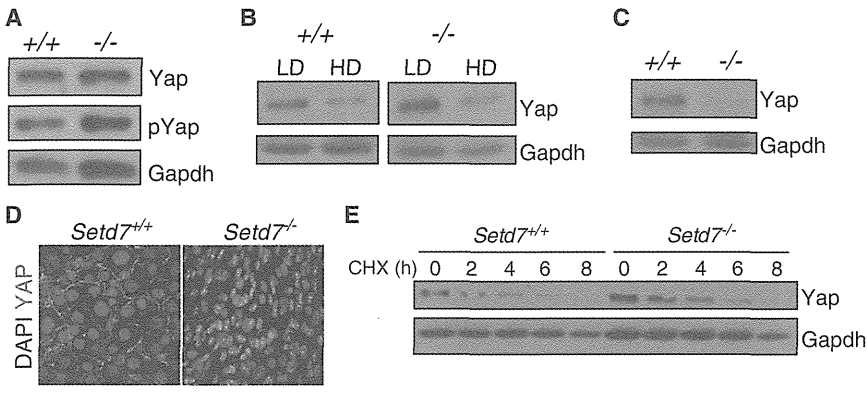

Figure 3. Set7 Does Not Control Phosphorylation or Degradation of Yap

(A) *Setd7*$^{+/+}$ or *Setd7*$^{-/-}$ MEFs were grown to confluence, and whole cell extracts were immunoblotted with antibodies against Yap, pYap S127, and Gapdh.

(B) Equal cell numbers were seeded in either a petri dish or six-well plate and lysed 24 hr later. Density-dependent Yap degradation was not affected by lack of Set7.

(C and D) High-density seeded cells were overgrown for an additional 48 hr (hyperconfluent), and Yap was (C) quantified and (D) localized.

(E) Kinetics of Yap degradation was determined by treating *Setd7*$^{+/+}$ and *Setd7*$^{-/-}$ MEFs with cycloheximide (CHX) for indicated hours, followed by immunoblotting of whole cell extracts with antibodies against Yap and Gapdh. Results are representative of more than three independent experiments.

revealed that Yap accumulates in the cytoplasm/membrane of *Setd7*$^{+/+}$ MEFs, whereas the remaining Yap in *Setd7*$^{-/-}$ MEFs was primarily nuclear (Figure 3D). Finally, to test degradation kinetics, we incubated high-density *Setd7*$^{+/+}$ and *Setd7*$^{-/-}$ MEFs in the presence of cycloheximide and followed Yap protein levels over time. We did not observe differences in the degradation kinetics of Yap between *Setd7*$^{+/+}$ and *Setd7*$^{-/-}$ MEFs (Figure 3E). Having a fully functional degradation pathway is the likely reason *Setd7*$^{-/-}$ mice are viable, and we do not observe a phenotype similar to mice that overexpress Yap or YapS127A (Camargo et al., 2007; Dong et al., 2007). Together, these results indicate that Set7 is required for cytoplasmic retention, but not degradation, of Yap.

To determine how Set7 regulates Yap localization, we examined whether Set7 interacted with Yap. Coimmunoprecipitation of native Yap from *Setd7*$^{+/+}$ MEFs cultured at high density demonstrated that Set7 was in a complex with Yap (Figure 4A), but not with Tead1 (Figure S3A). Because Set7 does not have a signal sequence to enter or leave the nucleus (Donlin et al., 2012), we hypothesized that Set7-Yap interactions were occurring in the cytoplasm. We found that Set7, like pYapS127, was present primarily in the cytoplasm of high-density (confluent) MEFs (Figure 4B), suggesting that Set7 binds Yap in the cytoplasm and that this is where Set7 likely acts to promote the cytoplasmic retention of Yap. When immunoprecipitated Yap was analyzed by immunoblotting with two distinct anti-methyl lysine antibodies (ab23366, recognizing both mono- and dimethylated lysine, and ab7315, recognizing primarily dimethylated lysine) we found that Yap was monomethylated in *Setd7*$^{+/+}$ MEFs but not in *Setd7*$^{-/-}$ MEFs (Figure 4A). These results, combined with our finding that Set7 forms complexes with Yap, suggested that Set7 could directly monomethylate Yap.

Mass spectrometric analysis of Yap immunoprecipitated from confluent HEK293 cells stably expressing a Flag-tagged version of Yap was performed. Targeted high-resolution multiple reaction monitoring of the Yap 488-498 peptide revealed that a single lysine residue (K494) is monomethylated (Figure 4C), consistent with the monomethyltransferase activity of Set7 (Xiao et al., 2003). Di- or trimethylation of Yap K494 could not be detected (Table S1). To directly test whether K494 was involved in the subcellular localization of Yap, we transfected *Setd7*$^{+/+}$ MEFs with Yap containing either a mutation of the methylation site K494 (K494R) or the adjacent lysine residue K497 (K497R). Strikingly, we observed increased Yap nuclear localization in MEFs transfected with Yap K494R but not K497R (Figures 4D and 4E), despite normal S127 phosphorylation (Figure 4G). We observed increased *Ctgf* expression in cells transfected with the YapK494R mutant (Figure 4F). Although we cannot unequivocally rule out other potential methylation sites in Yap, our results indicate that monomethylation of Yap specifically at K494 is required for Yap cytoplasmic retention and function.

In this study, we have identified several phenotypes in *Setd7*$^{-/-}$ mice that suggest the involvement of Set7 in regulation of the Hippo pathway. One observation from our studies is that Set7 is a cytoplasmic protein in high-density grown MEFs, which could explain the normal levels of H3K4me1 observed in *Setd7*$^{-/-}$ MEFs (Lehnertz et al., 2011). Unlike most KMTs, Set7 does not have a nuclear export signal or nuclear localization signal (Donlin et al., 2012), and Set7 is the only methyltransferase that contains membrane occupation and recognition nexus repeats (Morn repeats) that are found in proteins linking the membrane to the cytoskeleton (Garbino et al., 2009). It is tempting to speculate that Set7 is located at cellular junctions where it would methylate and sequester Yap from nuclear entry and degradation. While phosphorylation of Yap by the upstream Hippo pathway kinases Lats1/2 has been shown to regulate cytoplasmic retention, our results demonstrate that Set7 is critical for the cytoplasmic sequestration of Yap through the monomethylation of K494. The molecular mechanisms of how Yap methylation controls cytoplasmic sequestration are unknown. The K494 methylation site in Yap is proximal to the carboxyl-terminal PDZ-binding domain, and methylation of this site may impinge upon Yap interactions with PDZ-dependent binding partners including Zona occludens-2 (Oka et al., 2010) and Nherf (Mohler et al., 1999). Furthermore, methylated Yap is a minority of the total cellular Yap protein, suggesting that Yap methylation is a dynamic process, and future studies to identify specific demethylases potentially involved in Yap localization are warranted. Finally, whether Hippo-pathway-dependent phosphorylation of Yap is required for Set7-dependent methylation remains

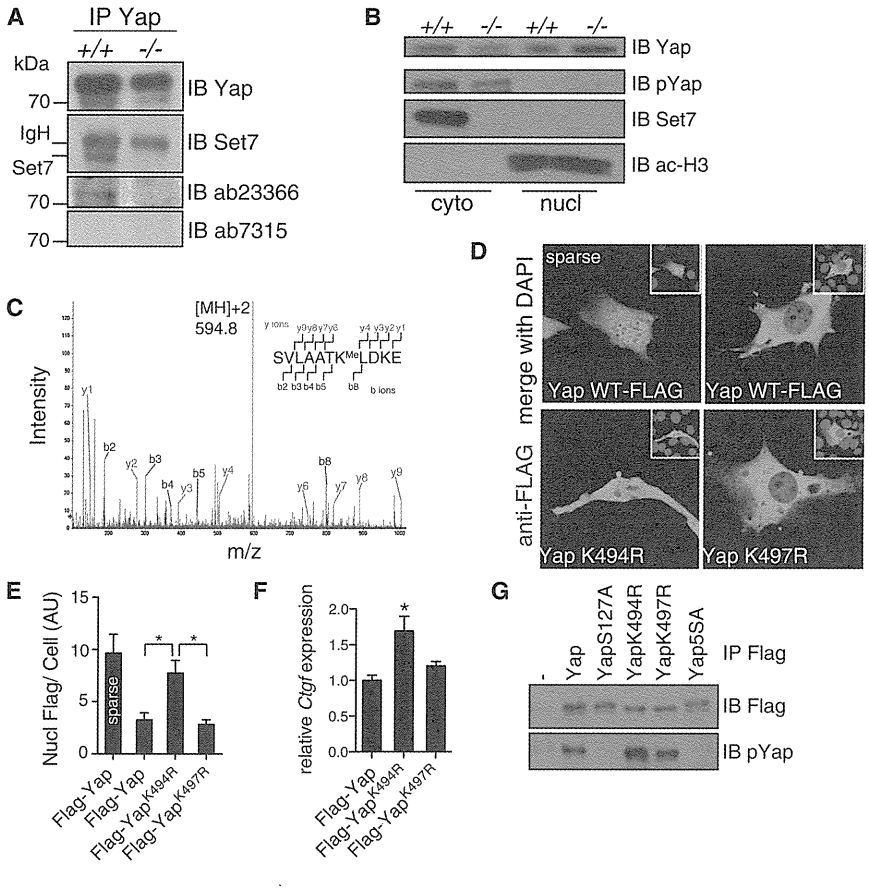

Figure 4. Set7 Monomethylates Yap on Lysine 494, and Lysine 494 Is Required for Cytoplasmic Retention

(A) Anti-Yap immunoprecipitates (IP) from high-density *Setd7*$^{+/+}$ and *Setd7*$^{-/-}$ MEFs were immunoblotted for Yap, Set7, methyl-lysine (mono-, dimethylated) (ab23366), and dimethyl-lysine (ab7315). IB, immunoblots.

(B) Cytosolic and nuclear fractions were isolated from high-density (confluent) cell cultures and probed for Yap, pYap, Set7, and Histone H3.

(C) Tandem mass spectrometry spectrum of Glu-C-digested Yap488-498 fragment (methylated K494 [MH]+2, mass 594.8 Da). Detected product ions are indicated in red (y ions) and blue (b ions).

(D) *Setd7*$^{+/+}$ MEFs were transfected with indicated Flag-Yap constructs, grown to confluence (unless indicated), and stained with a Flag-specific antibody followed by a fluorescent secondary antibody and DAPI.

(E) Nuclear Flag fluorescence was quantified.

(F) *Setd7*$^{+/+}$ MEFs were transfected with indicated plasmids, and *Ctgf* expression was measured of confluent cell cultures.

(G) HEK293 cells were transfected with indicated constructs, anti-Flag was used for IP, and IPs were immunoblotted using anti-Flag and anti-pYapS127. Data are presented as mean ± SEM and are representative of two to three experiments.

au, arbitrary units. *p < 0.05. See also Figure S3 and Table S1.

an open question. More generally, our finding that methylation is an important mechanism for controlling cytoplasmic/nuclear localization could have implications for other proteins that are regulated by subcellular localization.

EXPERIMENTAL PROCEDURES

Mice

Villin-Cre mice were obtained from Jackson Laboratories. *Setd7*$^{-/-}$ and *Setd7*$^{f/f}$ mice were described previously (Lehnertz et al., 2011). We did not observe any physiological effects from Cre expression. Animals were maintained in a specific-pathogen-free environment and tested negative for pathogens in routine screening. All experiments were carried out at the University of British Columbia following institutional guidelines.

IEC Isolation

IECs were isolated as previously described (Zaph et al., 2007). Briefly, intestines were opened lengthwise, washed in PBS containing penicillin and streptomycin, and cut into 1 cm pieces. IECs were obtained by shaking intestinal tissue in 2 mM EDTA in PBS for 20 min at 37°C twice. IECs were isolated, RNA was purified, and gene expression analyzed by quantitative PCR (qPCR).

Tissue Staining

Large intestines were fixed in formalin and paraffin-embedded. Tissue sections were stained with hematoxylin and eosin (H&E). Slides were analyzed on a Zeiss Axioplan2 microscope, and images were captured using a Qimaging Retiga EX CCD camera and Openlab 4.0.4 software (PerkinElmer). For immunofluorescence, 5 μm sections of paraformaldehyde-fixed, paraffin-embedded tissues were incubated with anti-Yap (Cell Signaling) followed by Alexa568-conjugated goat anti-rabbit and DAPI. Mice were injected with EdU 2 hr prior to sacrifice, and cecal sections were stained using Alexa568 Azide (Invitrogen) according to manufacturer instructions.

Cell Culture, Proliferation, and Transfection

MEFs were isolated and immortalized with SV40 as described previously (Lehnertz et al., 2011), and they were cultured in Dulbecco's modified Eagle's medium (DMEM) containing 10% fetal calf serum (FCS) and antibiotics, detached using trypsin (0.25%), and seeded at appropriate densities. Cells were counted after trypsin detachment using a hemocytometer. MEFs were transfected with plasmids encoding Flag-Set7, Flag-Set7^{H297G} (a point mutation that abolishes Set7 methyltransferase activity) (Nishioka et al., 2002; Tao et al., 2011), Flag-Yap, Flag-Yap^{K494R}, or Flag-Yap^{K497R} (Addgene "19045") (Oka et al., 2008; Hata et al., 2012) constructs using Lipofectamine 2000 (Invitrogen) according to the manufacturer's descriptions.

Yap Localization

Cells were seeded at different densities on tissue-culture-treated plastic chamber slides (ibidi GmbH) in DMEM + 10% FCS and incubated for 24 hr. Cells were then fixed in 4% paraformaldehyde for 20 min, permeabilized in 0.5% Triton X in PBS for 3 min, and blocked in 3% bovine serum albumin (BSA) in PBS for 20 min. Fixed cells were incubated with rabbit anti-Yap antibodies (Cell Signaling) in 3% BSA in PBS at a dilution of 1:200 for 40 min, washed five times for 5 min with PBS, and then incubated with secondary Alexa 488/568-conjugated goat anti-rabbit antibodies at a dilution of 1:400 for 20 min. Cells were again washed five times for 5 min with PBS, and then mounting media that contained DAPI (Invitrogen) was added before imaging with a confocal microscope (Olympus FV1000).

Statistical Analysis

Results represent the mean ± SEM. Statistical significance was determined by Student's t test or one-way analysis of variance with subsequent post hoc test.

SUPPLEMENTAL INFORMATION

Supplemental Information includes Supplemental Experimental Procedures, three figures, and one table and can be found with this article online at http://dx.doi.org/10.1016/j.devcel.2013.05.025.

ACKNOWLEDGMENTS

This work was supported by the Canadian Institutes of Health Research (CIHR; grants MSH-95368, MOP-89773, and MOP-106623 to C.Z., MOP-123433 to A.-C.G., and grant MOP-68865 to M.R.G.) and a Canada Foundation for Innovation grant (to C.Z.). The Structural Genomics Consortium is a registered charity (number 1097737) that receives funds from AbbVie, Boehringer Ingelheim, Canada Foundation for Innovation, the Canadian Institutes for Health Research (CIHR), Genome Canada through the Ontario Genomics Institute (OGI-055), GlaxoSmithKline, Janssen, Lilly Canada, the Novartis Research Foundation, the Ontario Ministry of Economic Development and Innovation, Pfizer, Takeda, and the Wellcome Trust (092809/Z/10/Z). The development of the mouse strains used in this study was supported by funds from the Leon Judah Blackmore Foundation (to F.M.V.R.). S.A.F. was supported by fellowships from the CIHR and the Michael Smith Foundation for Health Research (MSFHR). F.A. is the recipient of a CIHR/Canadian Association of Gastroenterologists (CAG)/Crohn's and Colitis Foundation of Canada postdoctoral fellowship. M.J.O. is the recipient of a CIHR/CAG/Janssen postdoctoral fellowship. C.H.A. holds a Canada Research Chair in Structural Genomics. F.M.V.R. is a Distinguished Scholar in Residence of the Peter Wall Institute for Advanced Studies. C.Z. is a CIHR New Investigator and an MSFHR Career Investigator.

Received: December 17, 2012
Revised: April 24, 2013
Accepted: May 28, 2013
Published: July 11, 2013

REFERENCES

Cai, J., Zhang, N., Zheng, Y., de Wilde, R.F., Maitra, A., and Pan, D. (2010). The Hippo signaling pathway restricts the oncogenic potential of an intestinal regeneration program. Genes Dev. *24*, 2383–2388.

Camargo, F.D., Gokhale, S., Johnnidis, J.B., Fu, D., Bell, G.W., Jaenisch, R., and Brummelkamp, T.R. (2007). YAP1 increases organ size and expands undifferentiated progenitor cells. Curr. Biol. *17*, 2054–2060.

Campaner, S., Spreafico, F., Burgold, T., Doni, M., Rosato, U., Amati, B., and Testa, G. (2011). The methyltransferase Set7/9 (Setd7) is dispensable for the p53-mediated DNA damage response *in vivo*. Mol. Cell *43*, 681–688.

Chuikov, S., Kurash, J.K., Wilson, J.R., Xiao, B., Justin, N., Ivanov, G.S., McKinney, K., Tempst, P., Prives, C., Gamblin, S.J., et al. (2004). Regulation of p53 activity through lysine methylation. Nature *432*, 353–360.

Cordenonsi, M., Zanconato, F., Azzolin, L., Forcato, M., Rosato, A., Frasson, C., Inui, M., Montagner, M., Parenti, A.R., Poletti, A., et al. (2011). The Hippo transducer TAZ confers cancer stem cell-related traits on breast cancer cells. Cell *147*, 759–772.

Dong, J., Feldmann, G., Huang, J., Wu, S., Zhang, N., Comerford, S.A., Gayyed, M.F., Anders, R.A., Maitra, A., and Pan, D. (2007). Elucidation of a universal size-control mechanism in *Drosophila* and mammals. Cell *130*, 1120–1133.

Donlin, L.T., Andresen, C., Just, S., Rudensky, E., Pappas, C.T., Kruger, M., Jacobs, E.Y., Unger, A., Zieseniss, A., Dobenecker, M.W., et al. (2012). Smyd2 controls cytoplasmic lysine methylation of Hsp90 and myofilament organization. Genes Dev. *26*, 114–119.

Ea, C.K., and Baltimore, D. (2009). Regulation of NF-kappaB activity through lysine monomethylation of p65. Proc. Natl. Acad. Sci. USA *106*, 18972–18977.

el Marjou, F., Janssen, K.P., Chang, B.H., Li, M., Hindie, V., Chan, L., Louvard, D., Chambon, P., Metzger, D., and Robine, S. (2004). Tissue-specific and inducible Cre-mediated recombination in the gut epithelium. Genesis *39*, 186–193.

Estève, P.O., Chin, H.G., Benner, J., Feehery, G.R., Samaranayake, M., Horwitz, G.A., Jacobsen, S.E., and Pradhan, S. (2009). Regulation of DNMT1 stability through SET7-mediated lysine methylation in mammalian cells. Proc. Natl. Acad. Sci. USA *106*, 5076–5081.

Garbino, A., van Oort, R.J., Dixit, S.S., Landstrom, A.P., Ackerman, M.J., and Wehrens, X.H. (2009). Molecular evolution of the junctophilin gene family. Physiol. Genomics *37*, 175–186.

Hata, S., Hirayama, J., Kajiho, H., Nakagawa, K., Hata, Y., Katada, T., Furutani-Seiki, M., and Nishina, H. (2012). A novel acetylation cycle of transcription co-activator Yes-associated protein that is downstream of Hippo pathway is triggered in response to SN2 alkylating agents. J. Biol. Chem. *287*, 22089–22098.

Heallen, T., Zhang, M., Wang, J., Bonilla-Claudio, M., Klysik, E., Johnson, R.L., and Martin, J.F. (2011). Hippo pathway inhibits Wnt signaling to restrain cardiomyocyte proliferation and heart size. Science *332*, 458–461.

Huang, J., and Berger, S.L. (2008). The emerging field of dynamic lysine methylation of non-histone proteins. Curr. Opin. Genet. Dev. *18*, 152–158.

Jenuwein, T., and Allis, C.D. (2001). Translating the histone code. Science *293*, 1074–1080.

Kanai, F., Marignani, P.A., Sarbassova, D., Yagi, R., Hall, R.A., Donowitz, M., Hisaminato, A., Fujiwara, T., Ito, Y., Cantley, L.C., and Yaffe, M.B. (2000). TAZ: a novel transcriptional co-activator regulated by interactions with 14-3-3 and PDZ domain proteins. EMBO J. *19*, 6778–6791.

Kouskouti, A., Scheer, E., Staub, A., Tora, L., and Talianidis, I. (2004). Gene-specific modulation of TAF10 function by SET9-mediated methylation. Mol. Cell *14*, 175–182.

Krummel, K.A., Lee, C.J., Toledo, F., and Wahl, G.M. (2005). The C-terminal lysines fine-tune P53 stress responses in a mouse model but are not required for stability control or transactivation. Proc. Natl. Acad. Sci. USA *102*, 10188–10193.

Kurash, J.K., Lei, H., Shen, Q., Marston, W.L., Granda, B.W., Fan, H., Wall, D., Li, E., and Gaudet, F. (2008). Methylation of p53 by Set7/9 mediates p53 acetylation and activity in vivo. Mol. Cell *29*, 392–400.

Lehnertz, B., Northrop, J.P., Antignano, F., Burrows, K., Hadidi, S., Mullaly, S.C., Rossi, F.M., and Zaph, C. (2010). Activating and inhibitory functions for the histone lysine methyltransferase G9a in T helper cell differentiation and function. J. Exp. Med. *207*, 915–922.

Lehnertz, B., Rogalski, J.C., Schulze, F.M., Yi, L., Lin, S., Kast, J., and Rossi, F.M. (2011). p53-dependent transcription and tumor suppression are not affected in Set7/9-deficient mice. Mol. Cell *43*, 673–680.

Mohler, P.J., Kreda, S.M., Boucher, R.C., Sudol, M., Stutts, M.J., and Milgram, S.L. (1999). Yes-associated protein 65 localizes p62(c-Yes) to the apical compartment of airway epithelia by association with EBP50. J. Cell Biol. *147*, 879–890.

Nishioka, K., Chuikov, S., Sarma, K., Erdjument-Bromage, H., Allis, C.D., Tempst, P., and Reinberg, D. (2002). Set9, a novel histone H3 methyltransferase that facilitates transcription by precluding histone tail modifications required for heterochromatin formation. Genes Dev. *16*, 479–489.

Oka, T., Mazack, V., and Sudol, M. (2008). Mst2 and Lats kinases regulate apoptotic function of Yes kinase-associated protein (YAP). J. Biol. Chem. *283*, 27534–27546.

Oka, T., Remue, E., Meerschaert, K., Vanloo, B., Boucherie, C., Gfeller, D., Bader, G.D., Sidhu, S.S., Vandekerckhove, J., Gettemans, J., and Sudol, M. (2010). Functional complexes between YAP2 and ZO-2 are PDZ domain-dependent, and regulate YAP2 nuclear localization and signalling. Biochem. J. *432*, 461–472.

Pan, D. (2010). The hippo signaling pathway in development and cancer. Dev. Cell *19*, 491–505.

Pradhan, S., Chin, H.G., Estève, P.O., and Jacobsen, S.E. (2009). SET7/9 mediated methylation of non-histone proteins in mammalian cells. Epigenetics *4*, 383–387.

Purcell, D.J., Jeong, K.W., Bittencourt, D., Gerke, D.S., and Stallcup, M.R. (2011). A distinct mechanism for coactivator versus corepressor function by

histone methyltransferase G9a in transcriptional regulation. J. Biol. Chem. *286*, 41963–41971.

Schlegelmilch, K., Mohseni, M., Kirak, O., Pruszak, J., Rodriguez, J.R., Zhou, D., Kreger, B.T., Vasioukhin, V., Avruch, J., Brummelkamp, T.R., and Camargo, F.D. (2011). Yap1 acts downstream of α-catenin to control epidermal proliferation. Cell *144*, 782–795.

Su, I.H., and Tarakhovsky, A. (2006). Lysine methylation and 'signaling memory'. Curr. Opin. Immunol. *18*, 152–157.

Tao, Y., Neppl, R.L., Huang, Z.P., Chen, J., Tang, R.H., Cao, R., Zhang, Y., Jin, S.W., and Wang, D.Z. (2011). The histone methyltransferase Set7/9 promotes myoblast differentiation and myofibril assembly. J. Cell Biol. *194*, 551–565.

van der Flier, L.G., and Clevers, H. (2009). Stem cells, self-renewal, and differentiation in the intestinal epithelium. Annu. Rev. Physiol. *71*, 241–260.

Wang, H., Cao, R., Xia, L., Erdjument-Bromage, H., Borchers, C., Tempst, P., and Zhang, Y. (2001). Purification and functional characterization of a histone H3-lysine 4-specific methyltransferase. Mol. Cell *8*, 1207–1217.

Xiao, B., Jing, C., Wilson, J.R., Walker, P.A., Vasisht, N., Kelly, G., Howell, S., Taylor, I.A., Blackburn, G.M., and Gamblin, S.J. (2003). Structure and catalytic mechanism of the human histone methyltransferase SET7/9. Nature *421*, 652–656.

Yang, X.D., Huang, B., Li, M., Lamb, A., Kelleher, N.L., and Chen, L.F. (2009). Negative regulation of NF-kappaB action by Set9-mediated lysine methylation of the RelA subunit. EMBO J. *28*, 1055–1066.

Yang, J., Huang, J., Dasgupta, M., Sears, N., Miyagi, M., Wang, B., Chance, M.R., Chen, X., Du, Y., Wang, Y., et al. (2010a). Reversible methylation of promoter-bound STAT3 by histone-modifying enzymes. Proc. Natl. Acad. Sci. USA *107*, 21499–21504.

Yang, X.D., Tajkhorshid, E., and Chen, L.F. (2010b). Functional interplay between acetylation and methylation of the RelA subunit of NF-kappaB. Mol. Cell. Biol. *30*, 2170–2180.

Zaph, C., Troy, A.E., Taylor, B.C., Berman-Booty, L.D., Guild, K.J., Du, Y., Yost, E.A., Gruber, A.D., May, M.J., Greten, F.R., et al. (2007). Epithelial-cell-intrinsic IKK-β expression regulates intestinal immune homeostasis. Nature *446*, 552–556.

Zhao, B., Wei, X., Li, W., Udan, R.S., Yang, Q., Kim, J., Xie, J., Ikenoue, T., Yu, J., Li, L., et al. (2007). Inactivation of YAP oncoprotein by the Hippo pathway is involved in cell contact inhibition and tissue growth control. Genes Dev. *21*, 2747–2761.

Zhao, B., Ye, X., Yu, J., Li, L., Li, W., Li, S., Yu, J., Lin, J.D., Wang, C.Y., Chinnaiyan, A.M., et al. (2008). TEAD mediates YAP-dependent gene induction and growth control. Genes Dev. *22*, 1962–1971.

Zhao, B., Li, L., Tumaneng, K., Wang, C.Y., and Guan, K.L. (2010). A coordinated phosphorylation by Lats and CK1 regulates YAP stability through SCF($^{\beta\text{-TRCP}}$). Genes Dev. *24*, 72–85.

Zhou, D., Zhang, Y., Wu, H., Barry, E., Yin, Y., Lawrence, E., Dawson, D., Willis, J.E., Markowitz, S.D., Camargo, F.D., and Avruch, J. (2011). Mst1 and Mst2 protein kinases restrain intestinal stem cell proliferation and colonic tumorigenesis by inhibition of Yes-associated protein (Yap) overabundance. Proc. Natl. Acad. Sci. USA *108*, E1312–E1320.